IEEE Access
Multidisciplinary | Rapid Review | Open Access Journal

Received November 25, 2019, accepted December 6, 2019, date of publication December 13, 2019,
date of current version December 23, 2019.

Digital Object Identifier 10.1109/ACCESS.2019.2959325

A Multilevel Image Thresholding Based on Hybrid Salp Swarm Algorithm and Fuzzy Entropy

HUSEIN S. NAJI ALWERFALI[1], MOHAMED ABD ELAZIZ[2], MOHAMMED A. A. AL-QANESS[3], AAQIF AFZAAL ABBASI[4], SONGFENG LU[5,6], FANG LIU[5], AND LI LI[7]

[1]School of Computer Science and Technology, Huazhong University of Science and Technology, Wuhan 430074, China
[2]Department of Mathematics, Faculty of Science, Zagazig University, Zagazig 44519, Egypt
[3]School of Computer Science, Wuhan University, Wuhan 430072, China
[4]Department of Software Engineering, Foundation University Islamabad, Islamabad 44000, Pakistan
[5]Shenzhen Huazhong University of Science and Technology Research Institute, Shenzhen 518063, China
[6]School of Cyber Science and Engineering, Huazhong University of Science and Technology, Wuhan 430074, China
[7]College of Mathematics and Statistics, Shenzhen University, Shenzhen 518060, China

Corresponding authors: Songfeng Lu (lusongfeng@hust.edu.cn) and Fang Liu (fang.liu@hust.edu.cn)

This work was supported in part by the Science and Technology Program of Shenzhen of China under Grant JCYJ20180306124612893, and in part by China Postdoctoral Science Foundation under Grant 2019M652647.

ABSTRACT The image segmentation techniques based on multi-level threshold value received lot of attention in recent years. It is because they can be used as a pre-processing step in complex image processing applications. The main problem in identifying the suitable threshold values occurs when classical image segmentation methods are employed. The swarm intelligence (SI) technique is used to improve multi-level threshold image (MTI) segmentation performance. SI technique simulates the social behaviors of swarm ecosystem, such as the behavior exhibited by different birds, animals etc. Based on SI techniques, we developed an alternative MTI segmentation method by using a modified version of the salp swarm algorithm (SSA). The modified algorithm improves the performance of various operators of the moth-flame optimization (MFO) algorithm to address the limitations of traditional SSA algorithm. This results in improved performance of SSA algorithm. In addition, the fuzzy entropy is used as objective function to determine the quality of the solutions. To evaluate the performance of the proposed methodology, we evaluated our techniques on CEC2005 benchmark and Berkeley dataset. Our evaluation results demonstrate that SSAMFO outperforms traditional SSA and MFO algorithms, in terms of PSNR, SSIM and fitness value.

INDEX TERMS Image segmentation, multi-level thresholding, salp swarm algorithm (SSA), moth-flame optimization (MFO).

I. INTRODUCTION

In recent years, SI methods received wide attention since they are applied in different areas and applications of Economics, Chemistry, and Medicine [1]. Moreover, the SI approaches are applied in different image processing fields, such as computer vision, face recognition, object identification, etc. Image segmentation can also be used in pre-processing stage of various applications, such as medical diagnosis [2] and satellite image processing [3]. Image segmentation is used to split an image into different classes with similar properties (such as texture, contrast, gray level, brightness, and color) and are based on a predefined criterion.

Recently, there are several approaches have been applied for image segmentation, including edge detection [4], clustering algorithms [5], threshold segmentation [6], and region extraction [7]. Threshold segmentation methods can be categorized in two categories, namely bi-level and multi-level segmentation. The bi-level methods groups image objects into two classes. If the number of classes is more than two, multi-level method is applied. The multi-level method splits an image's pixel into several classes based on the intensity [5]. Several existing studies used the image histogram to obtain the best threshold value by minimizing or maximizing the fitness functions, such as Kapur's entropy and Otsu.

However, the traditional models that have been used to find the optimal threshold value require more computational time. In order to address these limitations, meta-heuristic (MH) approaches have been used. In recent years, different MH algorithms have been applied in the field of image segmentation, such as the firefly optimization algorithm (FA) [8], harmony search (HS) algorithm [9], honey

The associate editor coordinating the review of this manuscript and approving it for publication was Jihwan P. Choi.

bee mating optimization (HBMO) [10], particle swarm optimization (PSO) [4], [6], [11], artificial bee colony (ABC) [12], [13], and cuckoo search (CS) algorithm [14].

In this paper, we present an alternative image segmentation model based on improving the performance of the salp swarm algorithm (SSA) using the moth flame optimization (MFO) algorithm. The proposed model is called (SSAMFO) and it aims to avoid the limitations in the traditional SSA through using the operators of the MFO as a local search to improve the group of followers. In general, both SSA and MFO are nature-inspired metaheuristic approaches and have been employed previously in various engineering problems and applications. SSA simulates the behavior of salp and it is applied as a global optimization method in [15] and established its performance. SSA was used in different research areas and applications, such as feature selection [16], [17], optimization tasks [18], automobile insurance fraud detection [19], passive sonar target classification [20] and wireless sensor networks (WSN) [21]. MFO can also be applied in various applications, such as feature selection [22], cloud computing [23], electricity consumption forecasting [24] and handwriting recognition [25]. Its main purpose was to solve mathematical problems, such as binary problems [26], multi-objective problems [27], and constraint-related issues [28].

In general, the proposed SSAMFO multilevel threshold image segmentation approach begins by computing the histogram of the given image. Then generate random integer solutions from the interval specified by the minimum and maximum value of the histogram. Each solution contains a set of values to represent the threshold values. To evaluate the quality of these solutions the fuzzy entropy is used as fitness function and the best solution has the largest fitness value. Thereafter, the current set of solutions is divided into leader and follower groups according to the same strategy used in traditional SSA. If the current solution belongs to the leader group, then all operators of SSA are used to update it, otherwise, the operators of the MFO is used. After finishing the updating process for all solutions, the terminal conditions are checked whether they are reached or not, so the previous steps are performed again. The output of the proposed SSAMFO is the optimal solution in this case. According to this strategy, the MFO is used to improve the followers having the largest effect on performance of SSA.

The main objectives of the performed study can be summarized as follows:

1) To propose an alternative image segmentation technique based on a modified salp swarm algorithm (SSA).
2) To improve the performance of the followers group in SSA using the operators of moth-flame optimization (MFO) algorithm.
3) To evaluate the performance of the proposed SSAMFO using fifteen global optimization problems.
4) To evaluate the performance of the SSAMFO using a set of eleven images and compared them with a set of popular image segmentation methods.

The rest of the paper is organized as follows. Section II summarizes the contributions of related developments. In Section III, we describe the preliminaries of the SSA and MFO, followed by the proposed method in section IV. Section V presents the experiment, evaluation, and comparison results. Finally, Section VI concludes the study.

II. RELATED WORK

The image segmentation is considered as one of the most important step in computer vision and image processing. Therefore, it has been applied in different fields, for example, remote sensing [29], medical imaging [30], and historical documents [31]. In general, the image segmentation is defined as the operation of grouping homogeneous pixels of the image in one class. There are many techniques to perform this task [32]–[35]. For example,

to classify the non-tumor and tumor images, also, to segment tumor region in CT images, Ramakrishnan and Sankaragomathi [7] first applied the support vector machine (SVM) classifier, then the segmentation was performed by the modified region growing (MRG) with a prediction threshold using grey wolf optimization (GWO).

In [36], the authors present a survey on recent document image segmentation methods. Since 2008, we witnessed an enormous increase in the research on this particular area.

Furthermore, there are several meta-heuristic approaches for image segmentation which simulate the behavior of swarm, biological, and physical laws. For example, genetic algorithm (GA) [37], differential evolution (DE) [38], PSO [12], ABC [39], electromagnetism optimization (EM) [40], and gravitational search algorithm (GSA) [41].

In [12], a hybrid differential evolution algorithm is presented. It used to select optimal threshold value for gray-level images by using Otsu function to define the criterion. This method defined a strategy adopted from the CS with DE. The primary idea of this algorithm is to switch between a mutation operator and a reset strategy by using a levy flight on the best individual to optimize the within-class variance introduced by Otsu. The proposed algorithm has better performance than CS, DE, ABC and self-adaptive differential evolution (SADE). Hussein et al. [42] presented an improved bees algorithm (BA) for multilevel image thresholding, namely PLBA. The main function of the proposed algorithm is to obtain optimal values of the threshold by maximizing Kapur's entropy and between class-variance. It has two main search steps: a local search and a global search feature. The local search applies greedy levy local algorithm [43], which is based on the levy flight operator. Whereas the global search incorporates path levy in the initialization phase that is employed in PLIA. Evaluation results determine that PLBA had better performance than other algorithms.

In [44], the authors presented a modified firefly algorithm (MFA) which applied for MTI segmentation. The proposed algorithm was applied by minimizing cross-entropy, Kapur entropy, and intra-class variance. They compared MFA with the firefly algorithm (FA), Levy search based FA (LFA), and Brownian search based FA (BFA). The comparison

results showed that the performance of MFA is better than FA, LFA, and BFA. An efficient method is presented by [45] to solve the multilevel threshold problem based on GWO. GWO is a nature-inspired algorithm that mimics the hunting and social behavior of the grey wolves that generally rely on their leadership hierarchy and hunting actions. Optimal values of the threshold are selected by using both Otsu's between-class variance and criteria Kapur's entropy. The evaluation results approved that GWO outperforms both bacterial foraging optimization (BFO) and PSO. Also, the GWO computational complexity is reduced due to the fast implementation of GWO.

In [1], authors applied two MH algorithms for multilevel threshold segmentation, namely MFO and whale optimization algorithm (WOA). The candidate solutions in the proposed algorithms are generated using the image histogram. These solutions are estimated using Otsu's fitness function. The evaluation experiment showed the superiority of MFO which outperforms WOA. Resma and Nair [46] presented an MIT algorithm, namely krill herd optimization (KHO) to solve image segmentation problems. In this method, optimal threshold values of image segmentation were evaluated by maximizing the Otsu and Kapur measures. The authors used various benchmark images to test the performance of KHO algorithm and compared it with several metaheuristics. Evaluation results showed that KHO outperforms several algorithms, such as PSO, MFO, and GA. In [47], the authors proposed an improved GSA, called GSA-GA (a hybrid algorithm of GSA with GA). The proposed method utilize the mutation operator and the roulette selection of the genetic algorithm which is integrated into the GSA. GSA-GA had been evaluated by using various numbers of thresholds on six test images and compared to the state-of-art methods. The results demonstrate its superiority on entropy and between-class variance criteria. In [48], authors presented an image segmentation method namely MCET-CSA. The main idea of this method is to integrate the minimum cross-entropy thresholding (MCET) criterion with crow search algorithm (CSA). It was applied to minimize the cross-entropy among classes. According to the evaluation results, MCET-CSA outperformed both harmony search (HS) and DE.

In [49], authors presented an MIT segmentation method using Otsu as the objective function. They presented a new method called chaotic bat algorithm (CBA). They also compared the proposed method with several state-of-art methods and it showed better performance.

To select the optimal threshold values, Samanta et al. [50] used Cuckoo Search (CS) which applied to reach the best solution. The proposed approach showed a good performance in terms of MSE and PSNR. In [51], the CS algorithm also was applied in MTI segmentation for color images and showed good performance. Dey et al. [52] presented a social group optimization (SGO) to support Kapur's and Otsu's multi-level thresholding. The proposed approach used for skin melanoma images and showed a good performance. Moreover, in [53], the SGO monitored Fuzzy-Tsallis entropy and ischemic stroke lesion (ISL) applied to segment magnetic resonance image (MRI) images. The proposed method was compared to several previous methods and showed good performance. FA also shows good performance in different image segmentations [54], including RGB color images [55]. Raja [56] presented an MIT approach using firefly algorithm. They used Otsu's as the objective function. FA showed good performance compared to other methods. Rajinikanth et al. [57] applied PSO and bacterial foraging optimization (BFO) to address MTI problem. Eight images had been used to test the proposed method in both bi-level and multilevel segmentation. The proposed method achieved good performance in all tests. Also, in [58], an entropy based MRI segmentation method was proposed using teaching learning based optimization (TLBO) algorithm.

III. METHODOLOGY

A. PROBLEM DEFINITION OF MULTI-LEVEL THRESHOLDING

In this section, we discuss the definition of the MTI segmentation problem. Let's assume that I represents a given gray-scale image, so, it consists of $K+1$ groups. Therefore, the goal of MTI techniques is to find K threshold values $\{t_k, k = 1, 2, K\}$, in which I is required to be divided into sub-groups $(C_k, k = 1, 2, \ldots, K)$, as presented in Eq.(1):

$$\begin{aligned} C_0 &= \{I_{ij} \mid 0 \le I_{ij} \le t_1 - 1\}, \\ C_1 &= \{I_{ij} \mid t_1 \le I_{ij} \le t_2 - 1\}, \\ &\ldots \\ C_K &= \{I_{ij} \mid t_K \le I_{ij} \le L - 1\} \end{aligned} \tag{1}$$

where t_k is the k-th threshold, I_{ij} is the gray level of the image at the (i, j)-th pixel, and L is the total number of gray levels of the images.

The multi-level (ML) threshold problem can be expressed as a maximization problem that can be used to determine the optimal threshold as:

$$t_1^*, t_2^*, \ldots, t_K^* = \arg \max_{t_1,\ldots,t_K} Fit(t_1, \ldots, t_K) \tag{2}$$

where the objective function is Fit. In this study, we apply Fuzzy entropy function [59] as the objective function. It is one of the most popular techniques used in MTI segmentation problems [60]–[62]. It can be expressed as:

$$Fit(t_1, \ldots, t_K) = \sum_{k=1}^{K} H_i \tag{3}$$

$$H_k = -\sum_{i=0}^{L-1} \frac{p_i \times \mu_k(i)}{P_k} \times ln(\frac{p_i \times \mu_k(i)}{P_k}), \tag{4}$$

$$P_k = \sum_{i=0}^{L-1} p_i \times \mu_k(i) \tag{5}$$

$$\mu_1(l) = \begin{cases} 1 & l \le a_1 \\ \dfrac{l - c_1}{a_1 - c_1} & a_1 \le l \le c_1 \\ 0 & l > c_1 \end{cases} \tag{6}$$

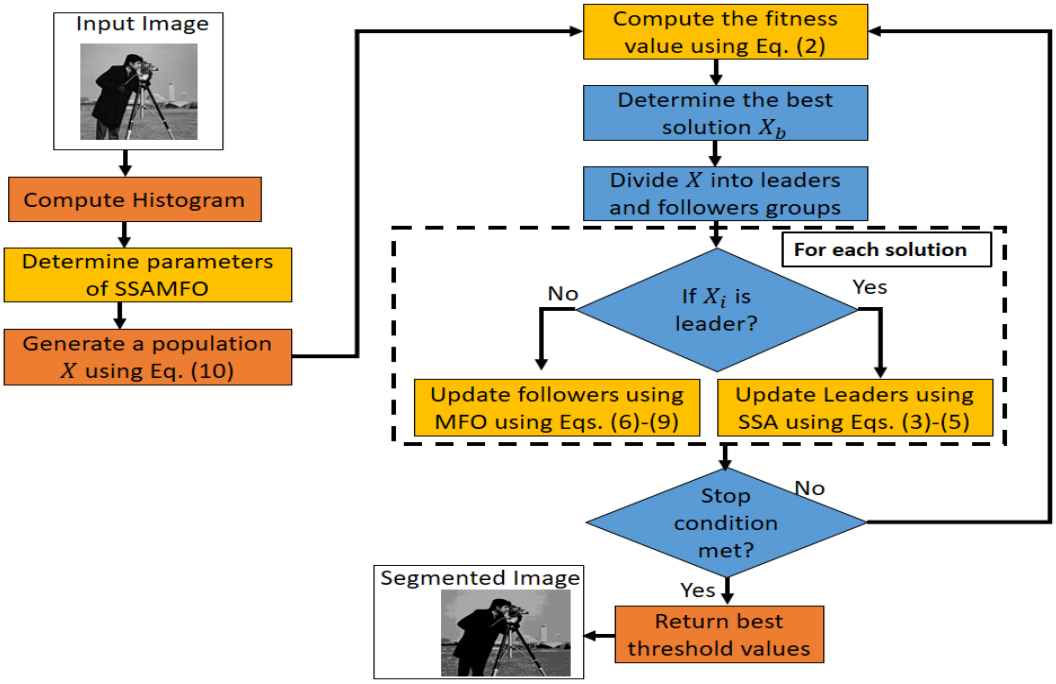

FIGURE 1. Proposed SSAMFO image segmentation method.

$$\mu_K(l) = \begin{cases} 1 & l \le a_{K-1} \\ \dfrac{l - a_K}{c_K - a_K} & a_{K-1} < l \le c_{K-1} \\ 0 & l > c_{K-1} \end{cases} \tag{7}$$

where $a_1, c_1, \ldots, a_{k-1}, c_{k-1}$ are the fuzzy parameters, where $0 \le a_1 \le c_1 \le \ldots \le a_{K-1} \le c_{K-1}$. The $t_1 = \frac{a_1+c_1}{2}, t_2 = \frac{a_2+c_2}{2}, \ldots, t_{K-1} = \frac{a_{K-1}+c_{K-1}}{2}$.

Moreover, the fuzzy entropy is used as fitness function in several image segmentation methods and applied to different applications, such as brain MRI segmentation [63], Brain tumor segmentation [64], color image [65], and others [66], [67].

B. SALP SWARM ALGORITHM (SSA)

SSA is a new nature-inspired optimization algorithm [15] which mimics the behavior of Salpidae's family. SSA is proposed to solve various optimization problems. Like other MH algorithms, it starts by generating a set of solutions with n dimensions. Solutions are divided into two main groups called leader (the salp in the front) and followers (the rest of salps). The n-dimensions determine the salp's position and they define the search space of the problem, where n is the problem variables. The leader position needs to be updated as the following equation:

$$X_j^1 = \begin{cases} X_b^j + c_1((UB_j - LB_j) \times c_2 + LB_j) & c_3 \le 0 \\ X_b^j - c_1((UB_j - LB_j) \times c_2 + LB_j) & c_3 > 0 \end{cases} \tag{8}$$

X_j^1 is the leader position in the j-th dimension, F_j is the food source in the j-th dimension, UB_j and LB_j are the upper and lower bounds, respectively. To maintain the search space, the parameters c_2 and c_3 are generated in random manner within the range [0, 1]. Where c_1 is a very important parameter because of its important balancing between exploration and exploitation phases, and it can be calculated as Equation (9):

$$c_1 = 2e^{-(\frac{4t}{t_{max}})^2}, \tag{9}$$

here, t represents current iteration, where t_{max} represents the max iterations' number. Thereafter, SSA begins updating followers' position as following:

$$X_j^i = \frac{1}{2}(X_j^i + X_j^{i-1}) \tag{10}$$

X_j^i is the i-th follower position in the j-th dimension, where i is greater than 1. Moreover, Algorithm 1 presents the SSA steps.

C. MOTH-FLAME OPTIMIZATION (MFO)

MFO is an MH nature-inspired method presented by [68]. It mimics the behavior of moth for path navigation. MFO starts by setting an initial value of N agents, each one has K decision features that represent of selected features $X_{i,j}(j = 1, \ldots, K)$.

As described in [68], MFO is represented using the following three parts:

$$MFO = (R, B, T) \tag{11}$$

R is the initialization stage, where a set of solutions is randomly generated, also, in this stage, the quality of each solution is calculated. Next, the best solution is determined and stored in *flames*.

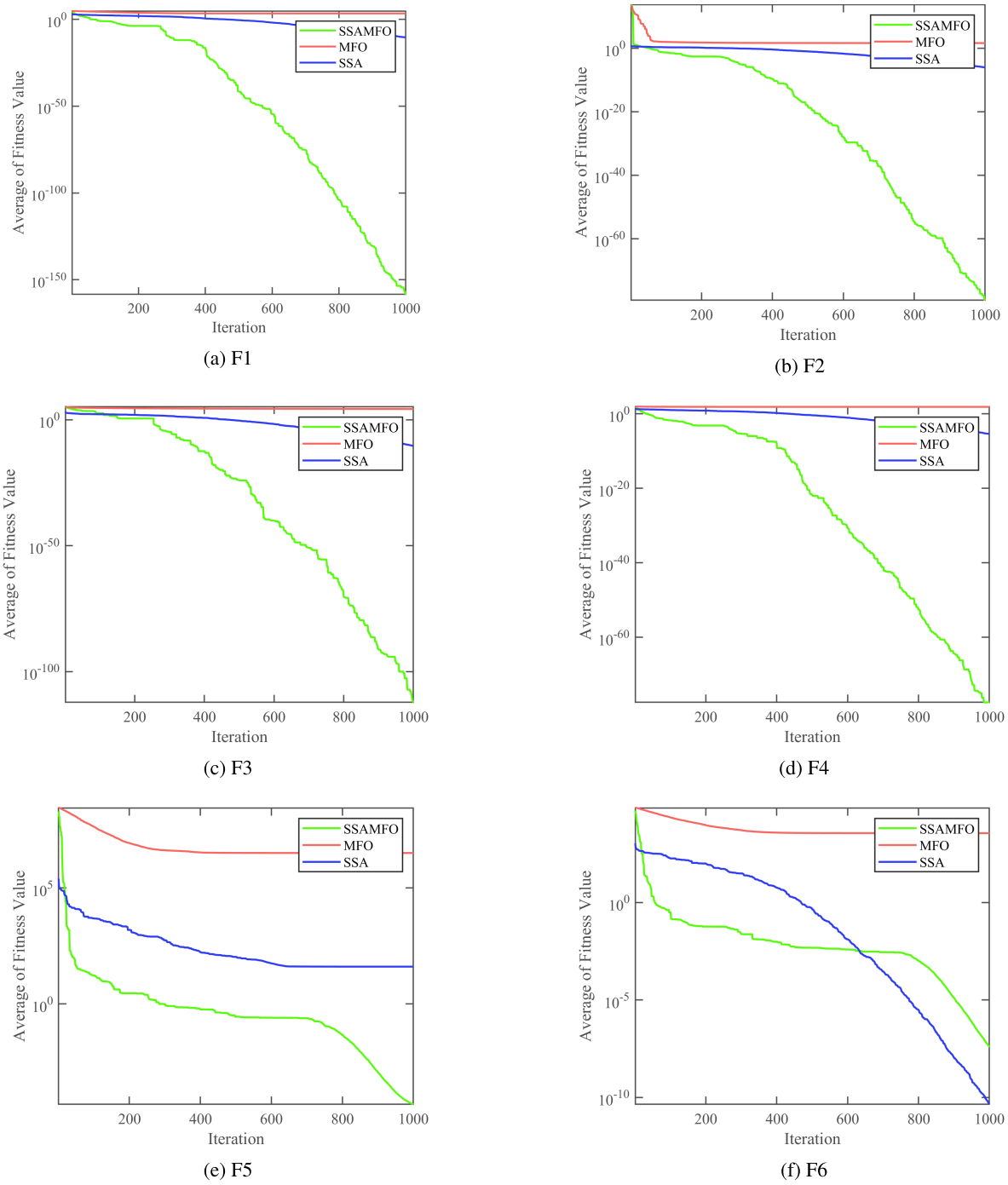

FIGURE 2. The fitness value of each method for functions F1-F6.

Furthermore, B is the updating stage, in which agents are updated using the operators, and T represents terminal conditions.

In the B stage, the position of agents is improved based on *flames* solution values, as presented in the following equations:

$$X_i = D_i \cdot e^{bl} \cdot cos(2\pi l) + F_u, \quad u = 1, 2, \ldots, N \tag{12}$$

$$D_i = |F_u - X_i|, \quad l \in [-1, 1] \tag{13}$$

where b is a constant value that is applied to find the shape of the logarithmic spiral.

As defined in [68], $Flames_N$ is decreased as following:

$$Flames_N = round(N - t \times \frac{N-1}{t_{max}}) \tag{14}$$

where t is the current iteration and t_{max} is the total number of iterations. The steps of the MFO algorithm are given in Algorithm 2.

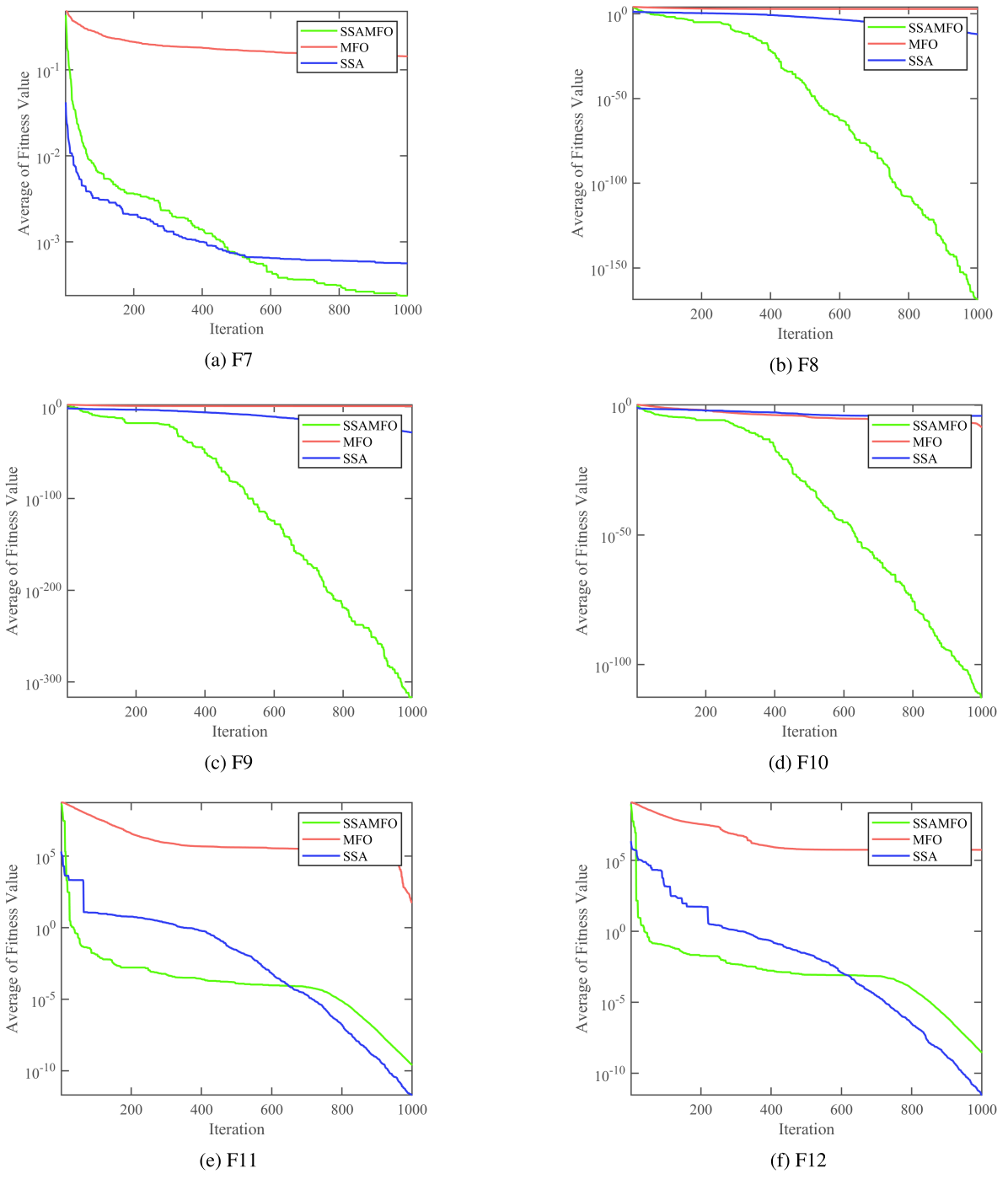

FIGURE 3. The fitness value of each method for functions F7-F12.

IV. PROPOSED METHOD

The framework of the SSAMFO approach as an image segmentation method is given in Figure 1. The proposed SSAMFO is a modified version of SSA using the operators of the MFO algorithm. It has been noticed that the follower's group has the largest effect on the performance of the traditional SSA. Therefore, the modification process is achieved by replacing the operators of the traditional SSA to update the position of followers by the operators of MFO.

The SSAMFO method starts by computing the histogram for the given image I then determine the initial value for N solutions (X) each of them (i.e., $X_i, i = 1, 2, \ldots, N$) has dimension K as defined in the following equation:

$$X_{i,j} = I_{min} + r_1 \times (I_{max} - I_{min}), \quad j = 1, 2, \ldots, K \quad (15)$$

where I_{min} and I_{max} represents the minimum and maximum gray value in the histogram of I, respectively. The next step is

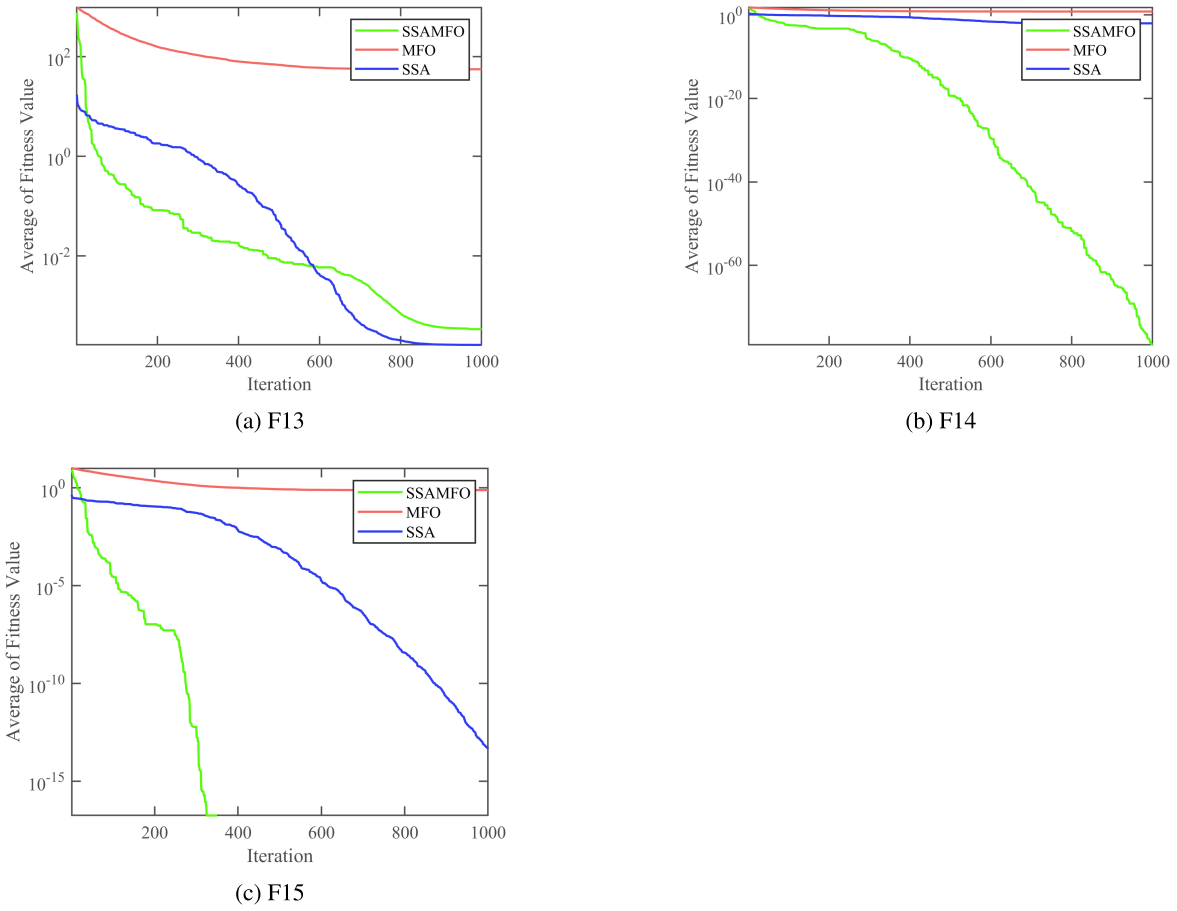

FIGURE 4. The fitness value of each method for functions F13-F15.

Algorithm 1 Salp Swarm Algorithm (SSA)

Initialize a population X.
while ($t < t_{max}$) **do**
  Calculate the fitness value for X_i.
  Determine the best solution (X_b).
  Using Eq. (9) to update c_1.
  for $i = 1 : N$ **do**
    if $i == 1$ **then**
      Update X_i using Eq. (8)
    else
      Update X_i using Eq. (10)
    end if
  end for
end while
Return X_b.

Algorithm 2 Moth-Flame Optimization (MFO)

Initialize a population X.
while ($t < t_{max}$) **do**
  Compute the fitness value X_i.
  Sort the moths and find the best (X_b).
  Update $Flames_N$ using Eq. (14)
  for $i = 1 : N$ **do**
    Update the position of moth using Eqs. (12)-(13)
  end for
end while
Return X_b.

to evaluate the quality of those initial solutions by computing the fitness value for each of them using Eq. (2).

The next process is to update the solutions using the operators of the SSAMFO and this starting by determining X_b which has the best fitness value Fit_b. Then solutions X are divided into two groups leader and followers similar to the traditional SSA. The operators of SSA is used to update the solutions in the leader group (as in Eqs. (8) and (10)), meanwhile, the operators of MFO will update the solutions in the followers group (as in Eqs. (11) and (14)).

The process of assessing and update the solutions is performed until the stop conditions reached (in this study, the total number of iterations is used).

A. COMPUTATIONAL COMPLEXITY

The computational complexity of SSAMFO is according to the complexity of the MFO and SSA. So, the complexity of


(a) Img1

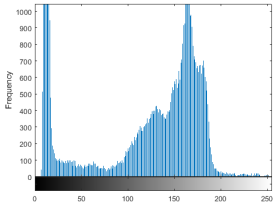
(b) Histogram of Img1


(c) Img2

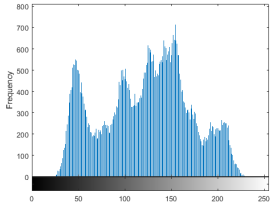
(d) Histogram of Img2


(e) Img3

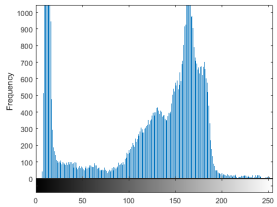
(f) Histogram of Img3


(g) Img4

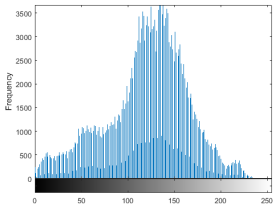
(h) Histogram of Img4


(i) Img5

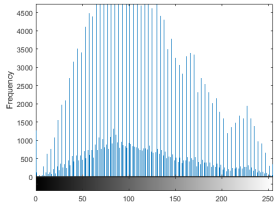
(j) Histogram of Img5


(k) Img6

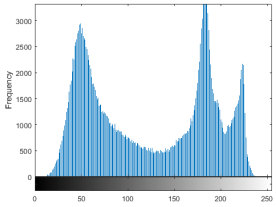
(l) Histogram of Img6

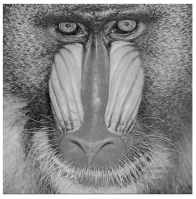
(m) Img7

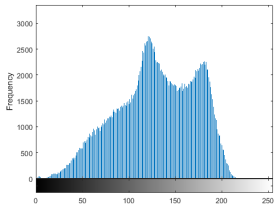
(n) Histogram of Img7


(o) Img8

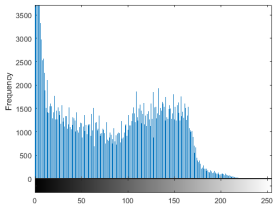
(p) Histogram of Img8


(q) Img9

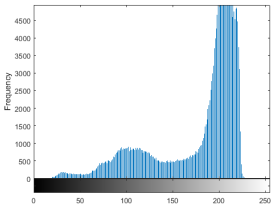
(r) Histogram of Img9

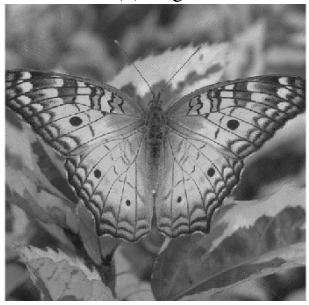
(s) Img10

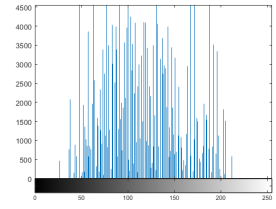
(t) Histogram of 10


(u) Img11

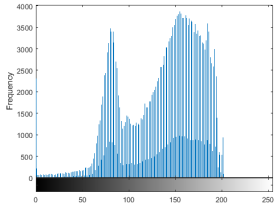
(v) Histogram of Img11

FIGURE 5. Tested images and their histograms.

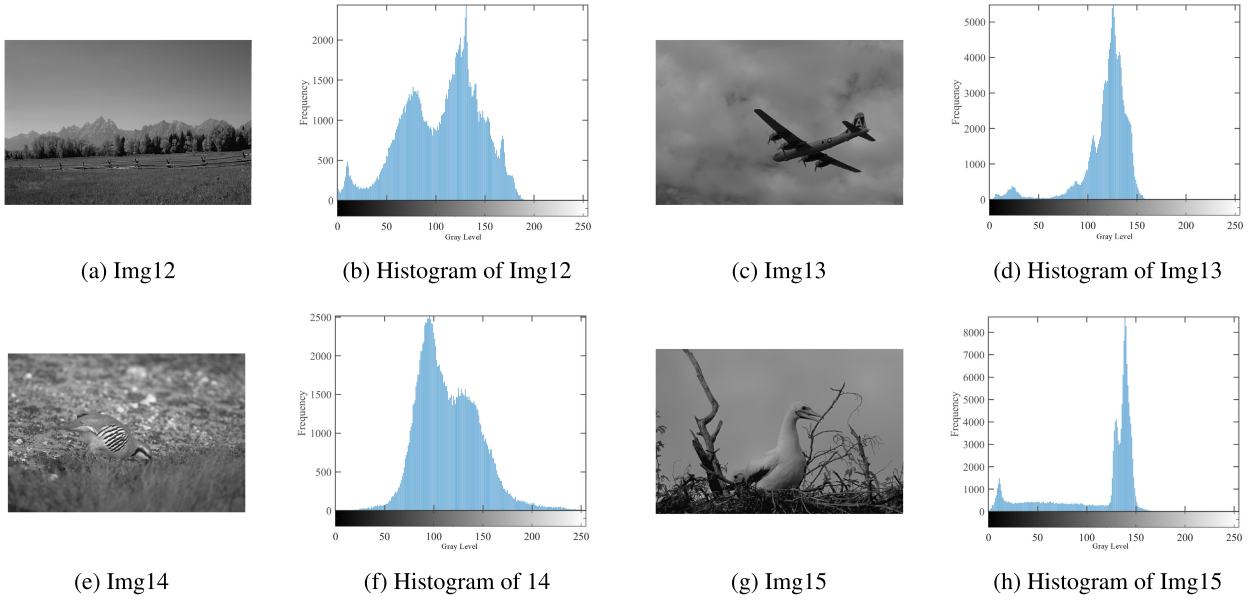

(a) Img12 (b) Histogram of Img12 (c) Img13 (d) Histogram of Img13

(e) Img14 (f) Histogram of 14 (g) Img15 (h) Histogram of Img15

FIGURE 6. Tested images from Berkeley dataset and their histograms.

TABLE 1. The definition of CEC2005 Benchmark problems.

ID	Formula of function	LW	UW	dim_W	Type
F1	$f(x) = \sum_{i=1}^{n} x_i^2$	-100	100	30	Unimodal
F2	$f(x) = \sum_{i=1}^{n} \lvert x_i \rvert + \Pi_{i=1}^{n} \lvert x_i \rvert$	-10	10	30	Unimodal
F3	$f(x) = \sum_{i=1}^{n} (\sum_{j-1}^{i} x_i)^2$	-100	100	30	Unimodal
F4	$f(x) = max_i\{\lvert x_i \rvert, 1 \leqslant i \leqslant n\}$	-100	100	30	Unimodal
F5	$f(x) = \sum_{i=1}^{n-1} [100(x_{i+1} - x_i^2)^2 + (x_i - 1)^2]$	-30	30	30	Unimodal
F6	$f(x) = \sum_{i=1}^{n} ([x_i + 0.5])^2$	-100	100	30	Unimodal
F7	$f(x) = \sum_{i=1}^{n} ix_i^4 + random[0, 1]$	-1.28	1.28	30	Unimodal
F8	$f(x) = \sum_{i=1}^{n} ix_i^2$	-10	10	30	Unimodal
F9	$f(x) = \sum_{i=1}^{n} ix_i^4$	-1.28	1.28	30	Unimodal
F10	$f(x) = \sum_{i=1}^{n} \lvert x_i \rvert^{i+1}$	-1	1	30	Unimodal
F11	$f(x) = \frac{\pi}{n}\{10sin^2(\pi y_1) + \sum_{i=1}^{n-1}(y_i - 1)^2[1 + 10sin^2(\pi y_{i+1})] + (y_n - 1)^2\} + \sum_{i=1}^{n} u(x_i, 10, 100, 4)$ $u(x_i, a, k, m) = \begin{cases} k(x_i - a)^m, & x_i > a \\ 0, & -a \leqslant x_i \leqslant a \\ k(-x_i - a)^m, & x_i < -a \end{cases}$	-50	50	30	Multimodal
F12	$f(x) = 0.1\{sin^2(3\pi x_1) + \sum_{i=1}^{n}(x_i - 1)^2[1 + sin^2(3\pi x_i + 1)] + (x_n - 1)^2[1 + sin^2(2\pi x_n)]\} + \sum_{i=1}^{n} u(x_i, 5, 100, 4)$	-50	50	30	Multimodal
F13	$f(x) = \sum_{i=1}^{n}(x_i - 1)^2 + [1 + sin^2(3\pi x_i + 1)] + sin^2(3\pi x_1) + \lvert x_n - 1 \rvert [1 + sin^2(3\pi x_n)]$	-10	10	30	Multimodal
F14	$f(x) = \sum_{i=1}^{n} \lvert x_i sin(x_i) + 0.1x_i \rvert$	-10	10	30	Multimodal
F15	$f(x) = 0.1n - (0.1\sum_{i=1}^{n} cos(5\pi x_i) - \sum_{i=1}^{n} x_i^2$	-1	1	30	Multimodal

SSAMFO is defined as:

$$O\,(SSAMFO) = \alpha O\,(SSA) + (N - \alpha) O\,(MFO) \quad (16)$$

where

$$O\,(SSA) = O\,(t_{max}\,(K \times N + EF \times N + N \log N))$$
$$O\,(MFO) = O\,(t_{max}\,(K \times N + EF \times N))$$

where EF is the number of fitness evaluations and N is the size of the population. α is the number of individuals updated using the operators of the traditional SSA.

V. EXPERIMENTS AND RESULTS

In this section, the performance of the proposed SSAMFO is evaluated by applying it to solve a set of global optimization problems from the CEC2005 benchmark. In addition, we determine the multilevel threshold values to segment a set of eleven images.

A. EXPERIMENTAL SERIES 1: GLOBAL OPTIMIZATION

This experimental series aims to test the performance of the SSAMFO as a global optimization method and compare it with the traditional SSA, and MFO algorithm.

1) DEFINITION OF 2005 BENCHMARK FUNCTIONS

In this section, the description of the CEC2005 benchmark problems [69] is discussed. We use fifteen problems which can be classified into two kinds (see Table 1) The first kind is unimodal, which has a single extreme point in the domain (F1-F10). Meanwhile, the second kind is multimodal, which has more than one global solution (F15-F19).

TABLE 2. Comparison resulst between SSAMFO, SSA, and MFO as global optimization method.

	Avgerage			STD			Best			Worst		
	SSAMFO	MFO	SSA	SSAMFO	MFO	SSA	SSAMFO	MFO	SSA	SSAMFO	MFO	SSA
F1	**3.2E-159**	2800.05	4.17E-11	**1.6E-158**	4582.544	2.84E-11	**2E-204**	0.000125	3.07E-12	**8E-158**	10000	1.19E-10
F2	**3.99E-80**	39.22343	9.17E-07	**1.51E-79**	20.95827	4.13E-07	**1E-110**	0.003017	2.52E-07	**7.14E-79**	70.00002	1.75E-06
F3	**6.1E-113**	18238.91	3.71E-11	**2.1E-112**	13082.01	2.72E-11	**4.5E-166**	916.7575	3.31E-12	**8E-112**	46251.87	1.05E-10
F4	**3.43E-78**	74.64607	4.24E-06	**1.72E-77**	7.189487	1.79E-06	**3.8E-107**	52.53843	9.44E-07	**8.58E-77**	85.78559	8.38E-06
F5	**4.73E-05**	3205702	40.61054	**5.78E-05**	15987014	116.8056	**2.88E-06**	53.54365	0.04835	**0.000195**	79943279	442.841
F6	3.78E-08	3620.098	**4.39E-11**	8.42E-09	7043.193	**3.8E-11**	2.14E-08	0.000127	**3.19E-12**	5.17E-08	20200.5	**1.58E-10**
F7	**0.000237**	0.143259	0.000564	**0.000257**	0.065556	0.000619	**1.82E-06**	0.057151	7.67E-05	**0.001051**	0.288575	0.00303
F8	**2E-169**	660.0002	8.99E-13	**0**	842.1203	6.32E-13	**1.3E-220**	0.000147	4.06E-14	**4.9E-168**	3600	2.07E-12
F9	**0**	3.435974	9.1E-29	**0**	10.69595	1.94E-28	**0**	1.99E-10	1.05E-31	**0**	53.68709	9.72E-28
F10	**2.8E-113**	3.11E-09	6.88E-05	**1.4E-112**	1E-08	9.54E-05	**3.3E-145**	1.19E-17	2.27E-06	**6.8E-112**	4.26E-08	0.000454
F11	2.44E-10	56.90585	**1.97E-12**	1.41E-10	266.8043	**1.81E-12**	8.92E-11	0.000115	**1.18E-13**	6.58E-10	1337.494	**8.05E-12**
F12	2.83E-09	558082.7	**2.94E-12**	1.02E-09	2790243	**2.17E-12**	1.36E-09	0.011984	**2.82E-13**	4.73E-09	13951247	**7.83E-12**
F13	0.000339	56.18722	**0.000165**	**0.000192**	87.93472	0.000201	2.64E-05	6.83E-05	**4.42E-06**	0.000833	315.2073	**0.000811**
F14	**9.3E-80**	6.644079	0.009843	**4.65E-79**	6.635905	0.018761	**7.5E-113**	9.42E-05	3.07E-08	**2.32E-78**	21.76085	0.084287
F15	**0**	0.765822	4.62E-14	**0**	0.55367	4.04E-14	**0**	0.147785	2.39E-15	**0**	2.086707	1.6E-13

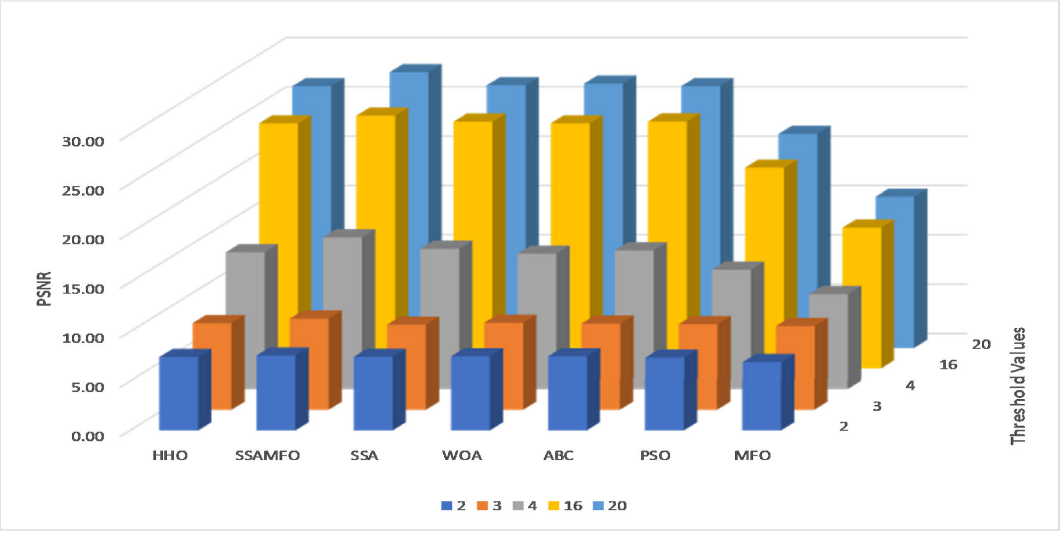

FIGURE 7. Average of the PSNR values overall tested images.

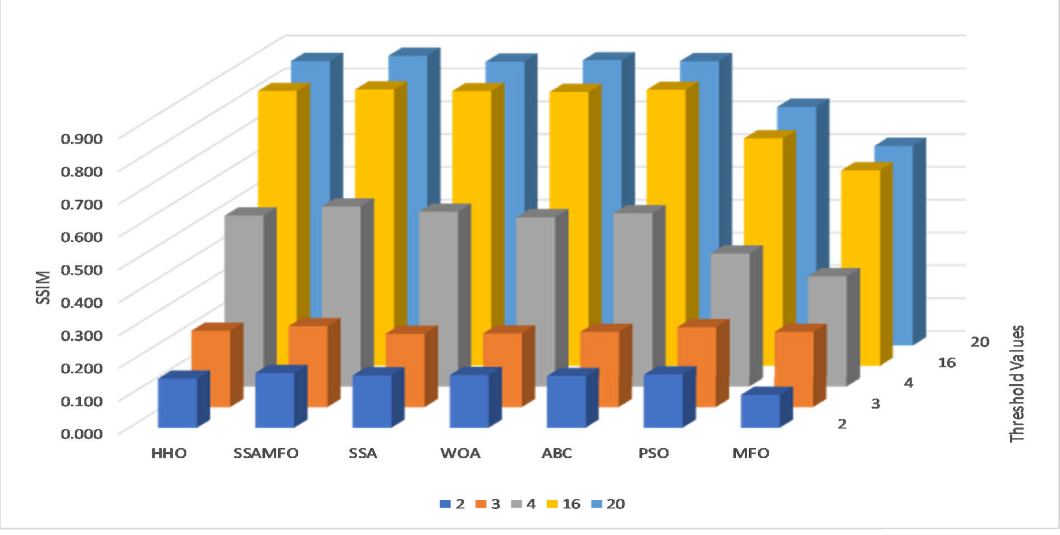

FIGURE 8. Average of the SSIM values overall tested images.

2) PERFORMANCE MEASURES

To evaluate the performance of the proposed SSAMFO approach as a global optimization method a set of measures are used. The metrics include the average (Avg_F), Worst value ($Worst_F$), Best ($Best_F$), and Standard deviation (STD_F) of the fitness value. These measures are

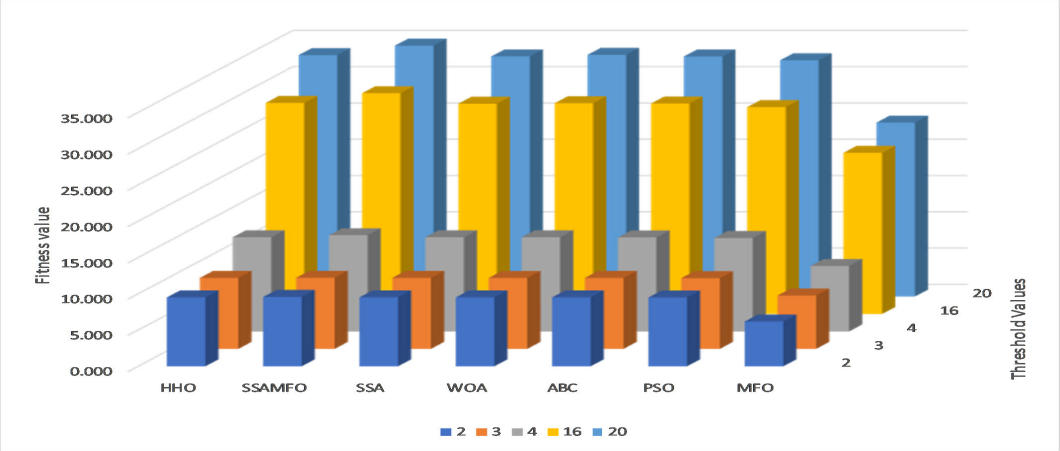

FIGURE 9. Average of Fitness value for each algorithm.

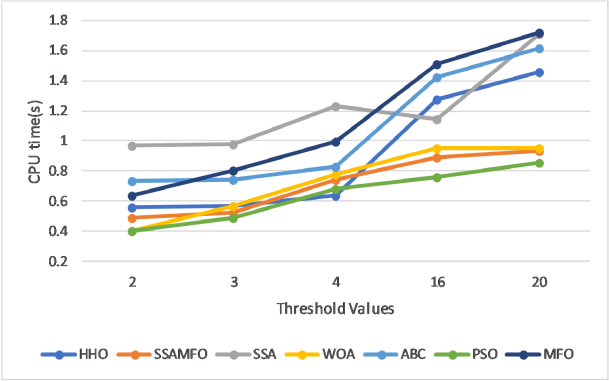

FIGURE 10. Average of CPU time(s) for each algorithm.

defined as:

$$Avg_F = \frac{1}{N_R}\sum_{i=1}^{N_R} Fit_{best}^{i} \tag{17}$$

$$Worst_F = \max_{1\le i\le N_R} Fit_{best}^{i} \tag{18}$$

$$Best_F = \min_{1\le i\le N_R} Fit_{best}^{i} \tag{19}$$

$$STD_F = \sqrt{\frac{1}{N_R-1}\sum_{i=1}^{N_R}(Fit_{best}^{i} - Avg_F)^2}, \tag{20}$$

In Eqs. (19)-(20), the N_R and Fit_{best} are the number of runs and the best fitness value, respectively.

3) RESULTS AND DISCUSSION

Table 2 and Figures 2-4 show the comparison results between our SSAMFO method and the traditional SSA, and MFO. From this table, it can be noticed that the SSAMFO outperforms other methods, according to the average fitness value, at most of the tested problems such as F1-F5, F7-F10, and F14-F15. However, the SSA is better than the MFO and SSAMFO at the rest functions. Additionally, it can be observed the high stability of the proposed SSAMFO since its STD value is better than the SSA and MFO nearly is all the tested functions except F6, FF11, and F12, the SSA is the better. The same observation can be noticed from the results of the worst and the best fitness value of each method. Moreover, Figures 2-4 depict the convergence curve for the SSAMFO, SSA, and MFO according to the tested functions. It can be seen that the proposed SSAMFO has the ability to convergence toward the global solution faster than the SSA, and MFO among all the functions except at F6, F11, F12, and F13, the SSA has better convergence than the others.

B. EXPERIMENTAL SERIES 2: IMAGE SEGMENTATION

To test the performance of SSAMFO method, a set of experiments is performed using different images [70]. The results are compared with the well-known MTI segmentation methods.

1) PERFORMANCE MEASURES

In this study, a set of image segmentation performance measures are used to assess the quality of the obtained threshold values. These measures are the Peak Signal-to-Noise Ratio (PSNR) [71], [72], and the Structural Similarity Index (SSIM) [73] and their definition are given as:

$$PSNR = 20log_{10}(\frac{255}{RMSE}) \tag{21}$$

where the root mean-squared error ($RMSE$) is represented as:

$$RMSE = \sqrt{\frac{\sum_{i=1}^{N_r}\sum_{j=1}^{N_c}(I_{i,j} - I_S i,j)^2}{N_r \times N_c}} \tag{22}$$

$$SSIM(I, I_S) = \frac{(2\mu_I\mu_{I_S} + c_1)(2\sigma_{I,I_S} + c_2)}{(\mu_I^2 + \mu_{I_S}^2 + c_1)(\sigma_I^2 + \sigma_{I_S}^2 + c_2)} \tag{23}$$

where $\mu_I(\sigma_I)$ and μ_{I_S} (σ_{I_S}) represent the images' mean intensity (standard deviation) of I and I_S), respectively. The σ_{I,I_S} is the covariance of I and I_S. The value of $c_1 = 6.5025$ and $c_2 = 58.52252$. Moreover, the fitness value is used to assess the quality of the threshold value and the CPU time(s) for each algorithm is used.

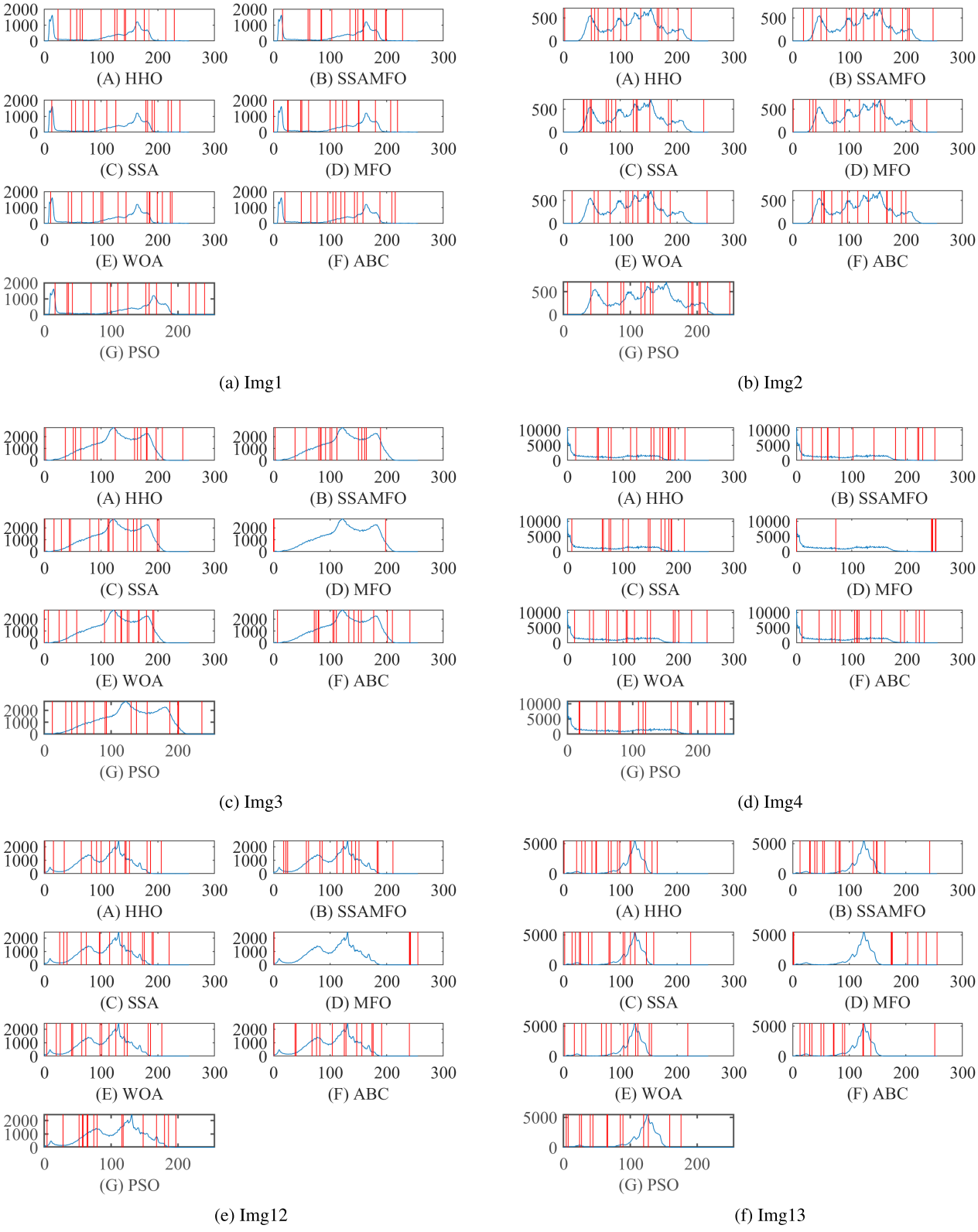

FIGURE 11. Threshold values over the histogram of images Img1-Img4,and Im12-Im13 at threshold level 16.

The proposed SSAMFO is compared with other six methods including Harris hawks optimization (HHO) [74], WOA [75], artificial bee colony (ABC) [76], PSO [77], SSA, and MFO. This comparison is performed with the size of the population 20, and the total number of iterations is 100.

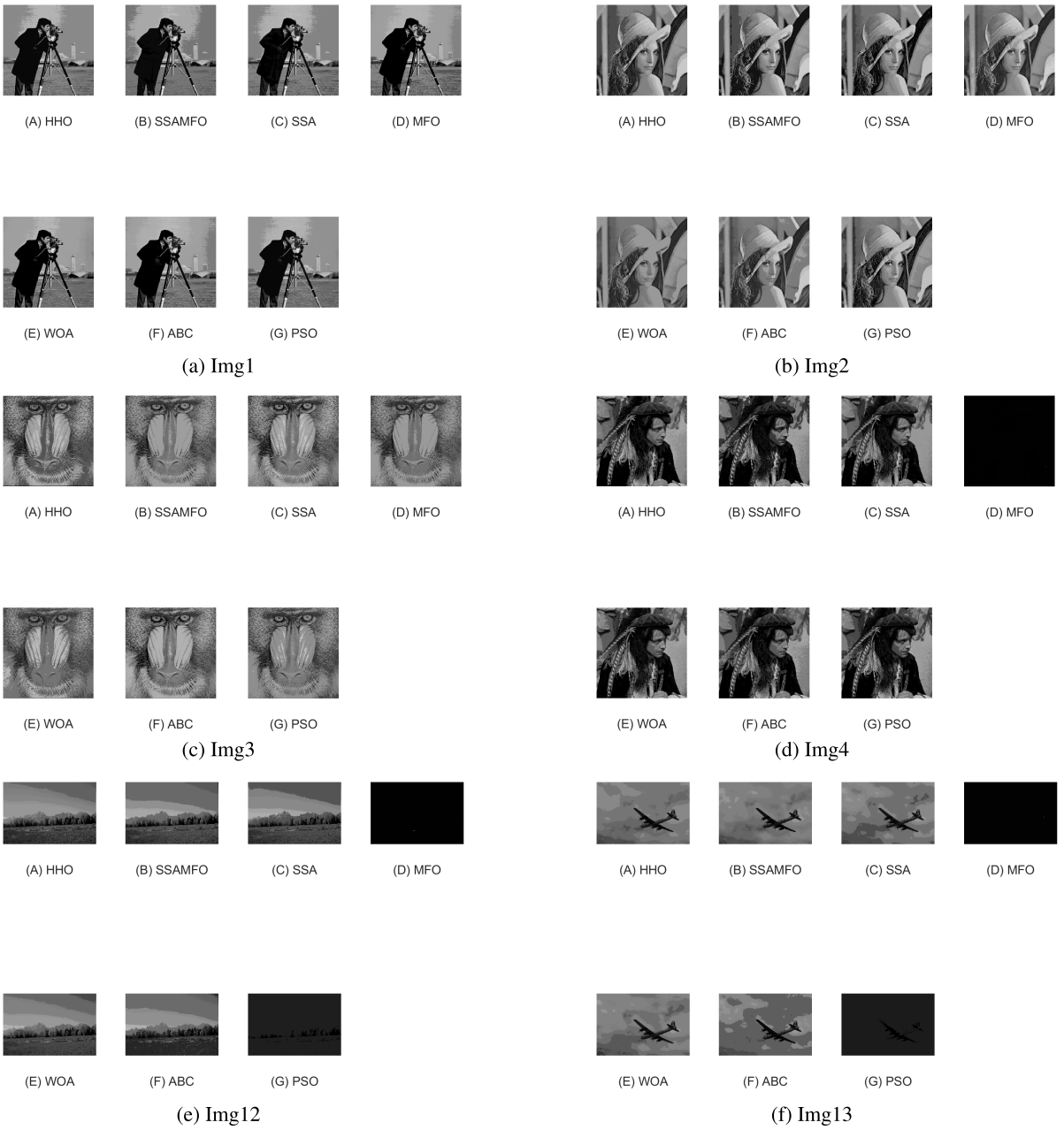

FIGURE 12. The Segmented images Img1-Img4, and Im2-Im13 at threshold level 16.

2) DATASET DESCRIPTION

We use a set of eleven images to assess the performance of the algorithms as image segmentation methods. These images have different characteristics, as represented by their histograms (see Figure 5-6).

3) RESULTS AND DISCUSSION

Here, the quality of each algorithm is evaluated at several threshold levels (i.e., 2, 3, 4, 16, and 20). In general, the high level of threshold values such as 16 and 20 are used to assess the quality of the algorithms at a high dimension since this is more suitable in different applications, such as remote sensing, cell images, and other images that contain several objects. Moreover, the performance of the SSAMFO is compared with several methods, including HHO, SSA, WOA, ABC, PSO, and MFO, as shown in Tables 3-5.

Table 3 shows the average of PSNR values overall the total number of runs among each threshold level. From the results given in this table, it can be noticed that the SSAMFO allocates the first rank with the highest PSNR value at 32 cases (boldface value). Followed by the WOA algorithm which provides better results than others. It can be seen that SSA and ABC have the highest value in four cases. In Figure 7 the average of PSNR values overall the tested images is presented. From this figure, it can be seen that the algorithms at

TABLE 3. PSNR value for each algorithm.

K	Img	HHO	SSAMFO	SSA	WOA	ABC	PSO	MFO
2	Im1	8.03	**8.26**	7.92	7.61	7.78	7.76	7.27
	Im2	7.40	**8.03**	7.76	7.53	7.73	7.32	7.14
	Im3	6.98	7.09	7.25	**7.32**	7.31	7.22	6.70
	Im4	10.08	**10.11**	9.66	9.89	9.98	9.81	9.40
	Im5	4.69	4.77	4.89	5.26	5.26	4.63	**5.40**
	Im6	7.15	**7.23**	6.91	6.89	7.09	7.73	6.63
	Im7	7.16	7.17	**7.69**	7.50	7.47	7.15	7.07
	Im8	6.48	6.33	6.21	**6.72**	6.48	6.67	5.79
	Im9	8.23	8.22	7.82	8.12	**8.39**	7.56	6.20
	Im10	7.98	**8.32**	7.95	8.13	7.91	7.91	8.06
	Im11	6.65	**7.25**	6.88	6.83	6.93	7.16	6.83
	im12	7.14	7.17	7.16	7.14	7.06	7.81	7.06
	im13	9.23	**9.23**	9.02	9.23	9.05	7.13	6.49
	im14	7.42	**7.64**	7.64	7.42	7.38	7.34	6.97
	im15	6.68	6.76	6.81	6.68	6.61	**7.18**	6.59
3	Im1	9.71	**9.72**	8.23	9.71	9.05	9.06	8.10
	Im2	8.98	8.59	8.72	8.85	8.46	8.77	**8.98**
	Im3	8.68	**8.74**	8.14	7.80	7.85	8.41	8.06
	Im4	10.83	**11.80**	10.84	11.03	10.92	11.12	9.05
	Im5	9.20	9.92	9.12	9.72	**11.13**	9.96	7.79
	Im6	8.70	**10.15**	8.16	8.69	9.06	8.37	8.36
	Im7	8.59	8.37	8.86	9.11	8.26	**9.17**	8.68
	Im8	7.72	7.37	7.51	**8.56**	7.98	7.61	7.92
	Im9	9.85	**10.79**	10.20	9.86	9.30	9.62	10.09
	Im10	9.49	**9.97**	8.92	8.39	9.26	9.68	8.67
	Im11	9.46	**9.86**	9.57	9.84	8.56	8.73	9.71
	im12	7.14	7.32	7.26	7.14	7.07	7.81	**8.23**
	im13	9.22	**9.88**	8.87	9.23	9.06	7.13	7.95
	im14	7.42	8.23	8.00	7.42	8.29	7.34	**8.88**
	im15	6.68	**7.76**	6.76	6.68	6.62	7.18	6.62
4	Im1	12.83	**15.74**	12.50	12.00	13.20	12.75	11.56
	Im2	13.07	**17.54**	13.45	13.22	13.21	14.11	12.91
	Im3	13.36	13.17	**13.65**	13.28	12.92	13.15	9.99
	Im4	14.51	**17.41**	15.06	15.16	15.05	14.82	12.07
	Im5	13.41	13.20	13.61	13.03	13.03	**13.87**	12.43
	Im6	13.22	13.62	**14.29**	13.65	13.50	14.22	11.12
	Im7	13.98	14.29	14.12	13.98	**14.33**	13.10	11.03
	Im8	14.52	**16.10**	14.15	14.02	14.44	14.78	7.31
	Im9	**13.27**	13.53	13.02	12.98	13.54	12.30	6.25
	Im10	14.61	**17.14**	14.23	13.67	13.92	13.78	9.76
	Im11	13.63	**16.52**	14.32	14.01	13.98	14.14	12.48
	im12	14.12	**14.54**	14.38	13.76	14.16	8.13	7.08
	im13	17.15	**18.31**	18.00	17.10	17.53	7.36	6.53
	im14	9.02	**10.42**	9.71	8.74	9.54	7.65	7.30
	im15	17.25	**19.02**	18.69	17.22	18.41	7.39	6.55
16	Im1	24.22	**25.82**	24.22	24.12	24.38	25.25	24.90
	Im2	23.92	24.15	24.39	24.22	24.38	24.50	**24.89**
	Im3	25.05	**26.82**	24.56	24.57	25.44	24.53	14.28
	Im4	25.10	**26.64**	25.34	25.50	25.59	24.95	10.83
	Im5	25.07	**26.56**	25.11	25.38	23.98	25.15	24.75
	Im6	24.17	**26.84**	23.97	23.73	24.77	23.91	8.88
	Im7	23.86	24.51	**24.83**	23.76	24.04	24.02	11.15
	Im8	25.36	25.26	25.08	**26.09**	25.73	25.40	11.65
	Im9	**24.33**	23.87	23.94	23.62	24.14	23.80	7.35
	Im10	25.24	25.88	25.27	24.81	**25.30**	23.71	24.68
	Im11	23.51	**25.71**	24.12	24.04	24.57	24.05	23.03
	im12	25.04	25.12	24.87	**25.68**	24.39	9.57	7.19
	im13	**28.37**	26.60	27.33	26.69	26.87	8.65	6.60
	im14	22.94	23.53	24.10	22.80	**24.19**	9.18	7.27
	im15	26.34	27.05	**28.11**	27.65	27.64	8.66	6.68
20	Im1	26.22	**28.73**	25.66	26.05	26.69	26.23	25.73
	Im2	26.05	27.38	25.83	**26.66**	25.73	25.50	25.12
	Im3	26.72	**27.33**	26.87	26.18	25.99	26.54	17.65
	Im4	26.61	**28.30**	26.91	26.73	27.02	26.20	11.44
	Im5	25.49	**28.23**	27.45	26.86	26.54	26.50	26.77
	Im6	25.92	28.41	25.68	25.90	25.46	**26.39**	8.22
	Im7	25.83	27.28	25.41	26.15	25.20	25.91	10.74
	Im8	**27.30**	27.09	26.50	27.30	26.75	26.94	14.98
	Im9	26.06	**26.63**	25.56	26.01	25.33	25.76	8.58
	Im10	26.15	**28.98**	25.89	26.49	26.80	25.54	26.87
	Im11	26.33	**27.93**	26.34	26.30	25.79	26.13	25.89
	im12	26.87	26.44	26.82	**27.99**	26.93	9.96	7.18
	im13	27.89	**30.12**	28.79	28.84	29.49	8.95	6.60
	im14	26.05	**26.81**	26.79	25.75	25.55	9.64	7.38
	im15	28.33	**29.25**	28.65	28.45	28.57	8.97	6.68

TABLE 4. SSIM values for each algorithm.

K	Img	HHO	SSAMFO	SSA	WOA	ABC	PSO	MFO
2	Im1	0.239	0.226	0.240	0.222	0.233	**0.264**	0.211
	Im2	0.156	**0.222**	0.192	0.177	0.197	0.159	0.140
	Im3	0.085	0.098	0.103	0.105	**0.105**	0.100	0.072
	Im4	0.224	0.231	0.214	**0.243**	0.214	0.215	0.176
	Im5	0.165	0.166	0.194	0.210	0.210	0.165	**0.224**
	Im6	0.210	0.236	0.210	0.176	0.221	**0.294**	0.150
	Im7	0.127	0.116	**0.166**	0.158	0.150	0.126	0.115
	Im8	0.154	**0.167**	0.133	0.147	0.163	0.167	0.045
	Im9	0.136	0.145	0.116	0.134	0.148	0.095	0.006
	Im10	0.174	**0.218**	0.191	0.210	0.168	0.175	0.163
	Im11	0.138	**0.183**	0.163	0.180	0.171	0.182	0.142
	im12	0.014	0.020	0.018	0.014	0.001	**0.127**	0.001
	im13	0.293	**0.297**	0.271	0.293	0.268	0.145	0.004
	im14	0.110	**0.133**	0.132	0.110	0.104	0.100	0.047
	im15	0.019	0.033	0.042	0.019	0.006	0.113	0.008
3	Im1	0.346	0.330	0.243	**0.357**	0.306	0.316	0.276
	Im2	0.268	0.235	0.243	0.252	0.233	0.261	**0.314**
	Im3	**0.203**	0.186	0.165	0.140	0.151	0.203	0.172
	Im4	0.260	0.278	**0.295**	0.270	0.253	0.270	0.107
	Im5	0.438	0.496	0.437	0.466	**0.579**	0.522	0.352
	Im6	0.293	**0.361**	0.274	0.308	0.311	0.308	0.286
	Im7	0.215	**0.251**	0.230	0.200	0.190	0.251	0.174
	Im8	0.240	**0.298**	0.210	0.214	0.251	0.241	0.161
	Im9	0.231	0.214	0.251	0.227	0.201	**0.285**	0.268
	Im10	0.273	0.217	0.243	0.185	0.256	0.272	**0.357**
	Im11	0.286	**0.314**	0.268	0.306	0.244	0.240	0.301
	im12	0.014	0.045	0.035	0.014	0.003	**0.127**	0.097
	im13	0.291	0.255	0.256	**0.292**	0.267	0.145	0.157
	im14	0.110	0.183	0.166	0.110	0.183	0.100	**0.409**
	im15	0.019	0.034	0.034	0.019	0.007	**0.113**	0.008
4	Im1	0.454	0.410	0.431	**0.478**	0.466	0.434	0.414
	Im2	0.468	**0.554**	0.494	0.467	0.477	0.528	0.454
	Im3	0.483	**0.497**	0.476	0.473	0.449	0.472	0.473
	Im4	0.392	**0.443**	0.423	0.426	0.427	0.405	0.346
	Im5	0.671	0.653	**0.674**	0.637	0.642	0.656	0.617
	Im6	0.545	0.568	**0.577**	0.560	0.549	0.571	0.493
	Im7	0.480	0.483	0.475	0.476	**0.489**	0.433	0.407
	Im8	0.557	0.573	0.561	0.555	0.552	**0.582**	0.457
	Im9	0.418	**0.443**	0.409	0.400	0.434	0.365	0.344
	Im10	0.504	0.526	0.487	0.461	**0.528**	0.461	0.380
	Im11	0.532	**0.558**	0.522	0.542	0.532	0.527	0.540
	im12	0.603	**0.619**	0.609	0.580	0.587	0.173	0.003
	im13	0.827	**0.857**	0.850	0.823	0.825	0.189	0.015
	im14	0.201	**0.314**	0.260	0.184	0.243	0.138	0.094
	im15	0.668	0.730	**0.731**	0.672	0.716	0.143	0.001
16	Im1	0.791	**0.831**	0.791	0.774	0.796	0.783	0.779
	Im2	0.824	0.827	0.827	0.832	0.831	0.836	**0.839**
	Im3	0.883	**0.893**	0.874	0.871	0.891	0.871	0.814
	Im4	0.770	0.767	0.782	0.769	**0.785**	0.754	0.709
	Im5	0.857	**0.876**	0.853	0.867	0.863	0.865	0.843
	Im6	0.808	0.811	0.814	0.807	**0.822**	0.801	0.808
	Im7	0.818	**0.825**	0.806	0.803	0.813	0.809	0.786
	Im8	0.829	0.837	0.828	**0.841**	0.837	0.823	0.813
	Im9	**0.855**	0.847	0.844	0.838	0.853	0.843	0.746
	Im10	0.832	**0.840**	0.827	0.825	0.836	0.803	0.819
	Im11	**0.838**	0.820	0.823	0.822	0.828	0.829	0.812
	im12	0.867	0.868	0.876	**0.879**	0.859	0.366	0.023
	im13	**0.906**	0.904	0.904	0.901	0.894	0.399	0.031
	im14	0.764	0.772	0.786	0.765	**0.796**	0.293	0.089
	im15	0.917	0.914	0.921	**0.922**	0.912	0.321	0.026
20	Im1	0.812	**0.851**	0.800	0.816	0.828	0.813	0.791
	Im2	0.866	0.862	0.857	**0.870**	0.862	0.851	0.831
	Im3	0.907	**0.928**	0.911	0.899	0.918	0.907	0.847
	Im4	0.805	0.806	0.802	0.806	**0.813**	0.794	0.722
	Im5	0.875	**0.895**	0.895	0.882	0.887	0.878	0.873
	Im6	0.838	0.834	0.833	0.836	0.829	**0.842**	0.745
	Im7	0.846	**0.897**	0.842	0.854	0.834	0.848	0.766
	Im8	0.865	**0.857**	0.847	**0.867**	0.850	0.856	0.823
	Im9	0.891	**0.948**	0.884	0.892	0.877	0.884	0.813
	Im10	0.854	**0.892**	0.847	0.861	0.863	0.842	0.866
	Im11	**0.864**	0.861	0.860	0.862	0.858	0.843	0.857
	im12	0.898	0.896	0.887	**0.908**	0.899	0.411	0.021
	im13	0.912	**0.920**	0.914	0.917	0.914	0.439	0.030
	im14	0.828	**0.847**	0.846	0.825	0.825	0.327	0.105
	im15	0.932	0.935	**0.936**	0.928	0.929	0.359	0.025

threshold level 2 nearly have the same PSNR value since this considered a simple multilevel threshold problem. However, at the threshold level 3 the HHO, SSAMFO, WOA, ABC, and PSO provide better results than the other two methods namely SSA and MFO. For threshold levels especially the higher levels(16 and 20) the proposed SSAMFO provides better results than the other methods.

According to the SSIM results given in Table 4, it can be noticed that the SSAMFO outperforms other approaches since it has the best SSIM at 25 cases from 55 cases which represent about 45%. Whereas, the ABC achieves the second

TABLE 5. Fitness value for each algorithm.

K	Img	HHO	SSAMFO	SSA	WOA	ABC	PSO	MFO
2	Im1	9.306	**9.326**	9.319	9.324	9.318	9.308	6.797
	Im2	10.042	10.045	10.040	10.038	10.015	**10.061**	5.227
	Im3	**10.004**	9.984	9.987	9.991	9.984	9.991	6.507
	Im4	9.819	**9.855**	9.850	9.821	9.841	9.845	8.408
	Im5	9.441	**9.454**	9.421	9.414	9.419	9.438	7.079
	Im6	10.150	10.143	**10.171**	10.156	10.152	10.129	6.147
	Im7	9.902	9.895	9.874	9.898	9.882	**9.909**	5.247
	Im8	9.462	**9.479**	9.478	9.439	9.476	9.453	6.982
	Im9	8.991	9.008	9.019	9.007	8.978	**9.027**	8.158
	Im10	8.948	8.949	**8.971**	8.947	8.947	8.963	5.275
	Im11	9.902	9.872	9.888	**9.914**	9.894	9.860	8.467
	im12	9.870	**9.867**	9.868	9.870	9.873	9.821	5.003
	im13	8.665	**8.994**	8.657	8.665	8.664	8.576	4.295
	im14	9.561	**9.829**	9.558	9.561	9.561	9.529	4.777
	im15	8.621	**8.918**	8.606	8.621	8.624	8.497	4.342
3	Im1	9.703	9.693	9.675	9.659	**9.727**	9.680	7.963
	Im2	10.408	10.404	10.426	10.404	**10.438**	10.434	9.158
	Im3	10.372	10.382	10.407	**10.438**	10.417	10.375	7.178
	Im4	10.207	10.191	10.202	10.148	10.195	**10.215**	9.435
	Im5	9.881	9.899	**9.912**	9.896	9.868	9.885	7.721
	Im6	10.514	10.534	**10.553**	10.519	10.500	10.543	9.186
	Im7	10.289	**10.306**	10.281	10.271	10.299	10.268	6.380
	Im8	9.864	**9.890**	9.870	9.823	9.852	9.875	6.145
	Im9	9.362	9.357	9.336	9.356	**9.388**	9.292	6.581
	Im10	9.315	9.368	**9.378**	9.355	9.340	9.298	6.945
	Im11	10.192	**10.239**	10.194	10.175	10.170	10.229	7.680
	im12	9.870	9.856	9.859	**9.870**	9.869	9.693	8.367
	im13	8.665	**8.763**	8.657	8.665	8.665	8.601	4.252
	im14	9.561	9.548	9.547	**9.561**	9.556	9.448	4.691
	im15	8.621	8.610	8.611	8.621	8.625	8.485	**8.710**
4	Im1	12.720	**12.733**	12.725	12.682	12.578	12.713	10.554
	Im2	13.432	13.399	13.422	**13.467**	13.432	13.337	10.001
	Im3	13.533	13.514	13.547	**13.555**	13.538	13.539	11.823
	Im4	13.328	13.294	13.333	**13.340**	13.315	13.337	9.366
	Im5	13.164	**14.140**	13.176	13.113	13.165	13.151	11.136
	Im6	13.706	13.695	13.712	**13.779**	13.690	13.759	12.326
	Im7	13.594	**14.579**	13.617	13.579	13.562	13.523	9.714
	Im8	12.569	12.541	**12.725**	12.589	12.660	12.563	9.460
	Im9	**12.133**	12.117	12.117	12.043	12.093	12.107	10.672
	Im10	11.513	**13.615**	11.505	11.560	11.487	11.544	11.042
	Im11	13.541	13.497	13.501	**13.563**	13.538	13.461	10.816
	im12	13.595	13.551	13.553	**13.619**	13.545	13.231	5.029
	im13	12.124	**12.544**	12.095	12.134	12.095	11.916	4.257
	im14	13.658	**13.690**	13.609	13.677	13.599	13.399	4.805
	im15	12.141	12.100	12.128	**12.149**	12.129	11.720	4.318
16	Im1	30.490	30.579	**30.686**	30.474	30.591	30.497	28.745
	Im2	29.237	**31.202**	29.194	29.486	29.193	29.444	29.117
	Im3	29.857	**30.102**	29.877	29.787	30.012	30.010	29.493
	Im4	31.096	30.904	30.957	30.984	30.909	30.960	29.666
	Im5	29.428	**32.495**	29.596	29.452	29.876	29.692	**30.714**
	Im6	30.925	31.176	30.974	31.082	**31.239**	31.116	30.433
	Im7	30.781	**31.889**	30.775	30.742	30.782	30.672	29.669
	Im8	26.442	26.143	26.660	26.107	26.405	26.387	**28.491**
	Im9	25.718	**31.584**	25.735	25.861	25.812	25.671	25.599
	Im10	21.828	**32.174**	21.723	21.300	21.794	21.559	21.951
	Im11	30.501	30.223	30.422	30.484	30.531	**30.586**	30.474
	im12	30.690	30.397	30.379	**30.744**	30.380	29.195	5.264
	im13	**28.268**	27.502	27.726	28.245	27.460	25.080	4.257
	im14	32.317	31.869	31.990	**32.590**	32.013	30.881	4.805
	im15	**29.001**	28.318	28.226	28.563	28.256	26.124	4.672
20	Im1	**35.446**	35.382	35.438	35.385	35.385	35.353	30.247
	Im2	33.446	33.131	33.273	33.040	33.153	33.214	**33.478**
	Im3	34.226	34.219	**34.404**	34.313	34.392	34.389	33.332
	Im4	35.777	**35.813**	35.727	35.777	35.750	35.615	34.673
	Im5	33.433	33.481	**33.976**	33.585	33.616	33.578	31.482
	Im6	**35.870**	35.809	35.685	35.722	35.815	35.815	31.115
	Im7	35.307	35.393	35.316	35.397	**35.552**	35.454	33.037
	Im8	29.685	**35.856**	29.629	29.808	29.727	29.745	29.330
	Im9	29.081	**33.642**	29.140	29.124	29.125	29.171	28.866
	Im10	23.767	**33.314**	23.606	23.903	23.910	24.032	23.855
	Im11	35.026	34.894	35.061	35.166	**35.390**	34.948	31.317
	im12	35.353	**35.966**	34.927	35.346	34.955	33.726	5.264
	im13	32.508	**32.756**	31.238	32.623	30.877	28.491	4.257
	im14	37.267	36.834	36.705	37.604	**36.600**	35.535	4.805
	im15	**33.081**	32.347	32.415	33.032	32.147	29.443	4.654

rank with seven cases followed by WOA, and PSO, which achieve the third and fourth rank, respectively. The rest set of algorithms nearly achieve the same number of good results. Moreover, from Figure 8 it can be noticed that the proposed SSAMFO and ABC at the low threshold level 2 nearly have the same SSIM. However, the PSO and SSAMFO at threshold level 3 have the same PSNR. From the threshold level 4 to the threshold level 20 the proposed SSAMFO provides higher SSIM values which indicate the high quality of the segmented images using the obtained threshold from it.

TABLE 6. Mean rank for each method using the Friedman test.

	HHO	SSAMFO	SSA	WOA	ABC	PSO	MFO
PSNR	3.9818	5.8727	4.0364	4.1273	4.0909	3.8364	2.0545
SSIM	4.2167	5.5417	3.7667	4.1500	4.5083	3.8667	1.9500
Fitness	4.1417	4.9750	4.7417	4.0333	4.3833	4.2917	1.4333

Table 5 and Figure 9 illustrate the comparison results between the proposed SSAMFO and the other methods. First, the function values at the levels threshold 2,3 and 4, the algorithms nearly have the same fitness value. However, the proposed SSAMFO has higher fitness value, at the levels threshold 16, and 20, than other methods. Additionally, it is noticed that the MFO has the smallest fitness value overall the tested threshold levels. But the SSA provides higher fitness value at the low threshold values (i.e, 2,3, and 4) and the ABC provides best fitness value at the high threshold levels (i.e., 16, and 20).

Figure 10 depicts the average of the CPU time(s) overall the tested images at each specific threshold level. It can be noticed that the PSO is considered as the fast algorithm, in this study, followed by the proposed SSAMFO that requires small CPU time(s) to reach the maximum number of iterations.

The segmented image and the thresholds values placement on the histogram of the images at threshold level 16 are given in Figure 11. On the resulting images, it can be seen the quality of the segmented image using the threshold obtained by the proposed SSAMFO method.

4) FRIEDMAN's TEST

For further analysis of the results of the proposed SSAMFO, Friedman test [78] is used. Friedman (FD) test is a non-parametric two-way analysis of variances by ranks, and it is a robust test to compare different algorithms over variant images. In the FD test, the high(low) rank indicates the corresponding method is the best when the measure assumes the largest (smallest) value is preferred. Table 6 shows the value of the mean rank of each method. It can be observed from these results that the proposed SSAMFO has the first rank according to the PSNR, SSIM, and Fitness value. This indicates the high quality of the segmented image results from the threshold values obtained by SSAMFO.

5) ROBUSTNESS OF THE PROPOSED SSAMFO

In this section, we evaluate the robustness of the proposed SSAMFO against the traditional SSA and MFO under different three values from Gaussian noise [79]. In this experiment, two images (i.e., im12, and im13) from Berkeley datasets are used and the same parameter setting used in the previous experiments is used. Table 7 shows the average of the PSNR and SSIM of the algorithms at two threshold values (3 and 16). From this table, we can observe that SSAMFO has higher quality as compared to the other two methods (i.e., SSA and MFO) in most of the cases. In addition, it can

TABLE 7. Robustness of SSAMFO under different three values of noise.

K	Noise	Img	PSNR			SSIM		
			SSAMFO	SSA	MFO	SSAMFO	SSA	MFO
3	0.1	Im12	7.156	**7.199**	6.525	0.110	**0.117**	0.101
		Im13	6.510	6.541	**6.768**	**0.158**	0.143	0.101
	0.05	Im12	**7.287**	7.162	6.019	0.133	0.129	**0.169**
		Im13	**6.802**	6.570	6.395	0.183	**0.195**	0.126
	0.03	Im12	**7.305**	7.198	6.407	0.143	0.149	**0.181**
		Im13	**8.564**	7.326	7.116	**0.206**	0.208	0.137
16	0.1	Im12	**22.978**	22.704	6.994	**0.824**	0.800	0.191
		Im13	**20.540**	20.068	6.412	**0.798**	0.774	0.216
	0.05	Im12	**23.984**	23.822	7.112	**0.837**	0.831	0.218
		Im13	22.228	**24.060**	6.517	**0.868**	0.853	0.258
	0.03	Im12	**24.829**	24.107	7.154	0.841	**0.849**	0.244
		Im13	25.884	**26.366**	6.579	**0.895**	0.882	0.292

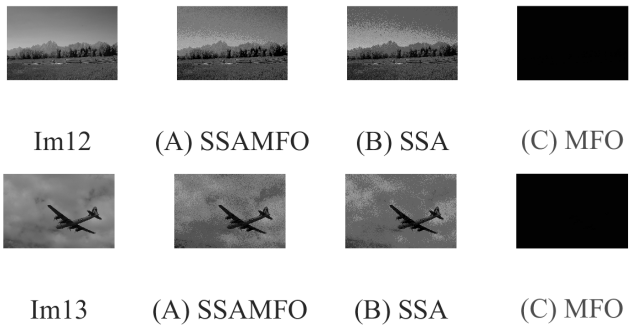

FIGURE 13. Segmented image at noise level ???.

be noticed that with increasing the level of noise the quality of the methods is decreased especially at threshold 3.

From all previously discussed results, it can be seen that the proposed SSAMFO has a high ability to find suitable threshold values to segment the given images. This results from combining the strengths of the MFO with SSA which gives the high ability to SSAMFO to avoid stagnation at the local point. However, the performance of SSAMFO can be improved further by selecting the suitable initial population using chaotic maps or opposite-based learning techniques. Moreover, similar to other multilevel image segmentation, there are some cases where SSAMFO algorithm cannot find suitable threshold values such as in Im5 and this represents the low-quality segmentation.

VI. CONCLUSION

This study presents an alternative image segmentation method using an improved version from the salp swarm algorithm (SSA). The proposed method depends on improving the solutions in the followers' group using the operators of the moth-flame optimization (MFO). Therefore, the developed method is named SSAMFO. To evaluate the performance of the SSAMFO, we perform a series of two different experiments. In the first experiment series, a set of fifteen global optimization problems from the CEC2005 benchmark were used to assess the ability of SSAMFO. In next step, we compare its results with SSA and MFO. The results demonstrate that SSAMFO has a higher ability to find a global solution for the CEC2005 benchmark problems. The second experimental series aims at assessing the SSAMFO as a segmentation method using a set of eleven images. The performance of the proposed SSAMFO was compared with several methods, including HHO, ABC, WOA, PSO, SSA, and MFO. The comparison results verified the high quality of the segmented images in terms of SSIM, PSNR, and Fitness value.

From the high-quality results achieved through the proposed SSAMFO technique, it can be applied in the future to several image segmentation applications problems for example, used the SSAMFO to threshold the RGB class images. Since, the RGB class thresholding is quite complex than gray (in RGB, every process is to be separately repeated for R, G, B channels).

Moreover, it can be applied to other fields, such as feature selection, cloud computing, and data clustering.

REFERENCES

[1] M. A. El Aziz, A. A. Ewees, and A. E. Hassanien, "Whale optimization algorithm and moth-flame optimization for multilevel thresholding image segmentation," *Expert Syst. Appl.*, vol. 83, pp. 242–256, Oct. 2017.

[2] S. Amerifar, A. T. Targhi, and M. M. Dehshibi, "Iris the picture of health: Towards medical diagnosis of diseases based on iris pattern," in *Proc. 10th Int. Conf. Digit. Inf. Manage. (ICDIM)*, Oct. 2015, pp. 120–123.

[3] A. K. Bhandari, A. Kumar, and G. K. Singh, "Tsallis entropy based multilevel thresholding for colored satellite image segmentation using evolutionary algorithms," *Expert Syst. Appl.*, vol. 42, no. 22, pp. 8707–8730, Dec. 2015.

[4] M. S. Chelva and A. K. Samal, "A comprehensive study of edge detection techniques in image processing applications using particle swarm optimization algorithm," in *Proc. IIRAJ Int. Conf. (ICCI-SEM-2K17)*. Bhubaneswar, India: GIFT, Feb. 2017, pp. 92–100. [Online]. Available: https://pdfs.semanticscholar.org/8256/8faeefe843bad025206b6dd80b9778ed14fe.pdf?_ga=2.259877069.690726289.1576255157-1153320948.1568283548

[5] A. Oliver, X. Munoz, J. Batlle, L. Pacheco, and J. Freixenet, "Improving clustering algorithms for image segmentation using contour and region information," in *Proc. IEEE Int. Conf. Automat., Qual. Test., Robot.*, vol. 2, May 2006, pp. 315–320.

[6] C. Qi, "Maximum entropy for image segmentation based on an adaptive particle swarm optimization," *Appl. Math. Inf. Sci.*, vol. 8, no. 6, p. 3129, 2014.

[7] T. Ramakrishnan and B. Sankaragomathi, "A professional estimate on the computed tomography brain tumor images using SVM-SMO for classification and MRG-GWO for segmentation," *Pattern Recognit. Lett.*, vol. 94, pp. 163–171, Jul. 2017.

[8] M. K. Alsmadi, "A hybrid firefly algorithm with fuzzy-C mean algorithm for MRI brain segmentation," *Amer. J. Appl. Sci.*, vol. 11, no. 9, pp. 1676–1691, 2014.

[9] D. Oliva, E. Cuevas, G. Pajares, D. Zaldivar, and M. Perez-Cisneros, "Multilevel thresholding segmentation based on harmony search optimization," *J. Appl. Math.*, vol. 2013, pp. 1–24, Art. no. 575414, doi: 10.1155/2013/575414.

[10] M.-H. Horng, "A multilevel image thresholding using the honey bee mating optimization," *Appl. Math. Comput.*, vol. 215, no. 9, pp. 3302–3310, Jan. 2010.

[11] L. Li and D. Li, "Fuzzy entropy image segmentation based on particle swarm optimization," *Prog. Natural Sci.*, vol. 18, no. 9, pp. 1167–1171, 2008.

[12] B. Akay, "A study on particle swarm optimization and artificial bee colony algorithms for multilevel thresholding," *Appl. Soft Comput.*, vol. 13, no. 6, pp. 3066–3091, 2013.

[13] U. Mlakar, B. Potočnik, and J. Brest, "A hybrid differential evolution for optimal multilevel image thresholding," *Expert Syst. Appl.*, vol. 65, pp. 221–232, Dec. 2016.

[14] S. Pare, A. Kumar, V. Bajaj, and G. K. Singh, "A multilevel color image segmentation technique based on cuckoo search algorithm and energy curve," *Appl. Soft Comput.*, vol. 47, pp. 76–102, Oct. 2016.

[15] S. Mirjalili, A. H. Gandomi, S. Z. Mirjalili, S. Saremi, H. Faris, and S. M. Mirjalili, "Salp Swarm Algorithm: A bio-inspired optimizer for engineering design problems," *Adv. Eng. Softw.*, vol. 114, pp. 163–191, Dec. 2017.

[16] H. Faris, M. M. Mafarja, A. A. Heidari, I. Aljarah, A.-Z. Ala'M, S. Mirjalili, and H. Fujita, "An efficient binary salp swarm algorithm with crossover scheme for feature selection problems," *Knowl.-Based Syst.*, vol. 154, pp. 43–67, Aug. 2018.

[17] R. A. Ibrahim, A. A. Ewees, D. Oliva, M. A. Elaziz, and S. Lu, "Improved salp swarm algorithm based on particle swarm optimization for feature selection," *J. Ambient Intell. Humanized Comput.*, vol. 10, no. 8, pp. 3155–3169, 2019.

[18] R. M. Rizk-Allah, A. E. Hassanien, M. Elhoseny, and M. Gunasekaran, "A new binary salp swarm algorithm: Development and application for optimization tasks," *Neural Comput. Appl.*, vol. 31, no. 5, pp. 1641–1663, 2019.

[19] S. K. Majhi, S. Bhatachharya, R. Pradhan, and S. Biswal, "Fuzzy clustering using salp swarm algorithm for automobile insurance fraud detection," *J. Intell. Fuzzy Syst.*, vol. 36, no. 3, pp. 2333–2344, 2019.

[20] M. Khishe and H. Mohammadi, "Passive sonar target classification using multi-layer perceptron trained by salp swarm algorithm," *Ocean Eng.*, vol. 181, pp. 98–108, Jun. 2019.

[21] H. M. Kanoosh, E. H. Houssein, and M. M. Selim, "Salp swarm algorithm for node localization in wireless sensor networks," *J. Comput. Netw. Commun.*, vol. 2019, pp. 1–12, Art. no. 1028723, doi: 10.1155/2019/1028723.

[22] L. Kumar and K. K. Bharti, "An improved BPSO algorithm for feature selection," in *Recent Trends in Communication, Computing, and Electronics*. Singapore: Springer, 2019, pp. 505–513.

[23] M. Ghobaei-Arani, A. A. Rahmanian, A. Souri, and A. M. Rahmani, "A moth-flame optimization algorithm for Web service composition in cloud computing: Simulation and verification," *Softw., Pract. Exper.*, vol. 48, no. 10, pp. 1865–1892, 2018.

[24] H. Zhao, H. Zhao, and S. Guo, "Using gm (1,1) optimized by MFO with rolling mechanism to forecast the electricity consumption of inner mongolia," *Appl. Sci.*, vol. 6, no. 1, p. 20, 2016.

[25] A. A. Ewees, A. T. Sahlol, and M. A. Amasha, "A bio-inspired moth-flame optimization algorithm for arabic handwritten letter recognition," in *Proc. Int. Conf. Control, Artif. Intell., Robot. Optim. (ICCAIRO)*, May 2017, pp. 154–159.

[26] S. Reddy, L. K. Panwar, B. K. Panigrahi, and R. Kumar, "Solution to unit commitment in power system operation planning using binary coded modified moth flame optimization algorithm (BMMFOA): A flame selection based computational technique," *J. Comput. Sci.*, vol. 25, pp. 298–317, Mar. 2018.

[27] S. J. Nanda, "Multi-objective moth flame optimization," in *Proc. Int. Conf. Adv. Comput., Commun. Inform. (ICACCI)*. Vikas, Sep. 2016, pp. 2470–2476.

[28] N. Jangir, M. H. Pandya, I. N. Trivedi, R. Bhesdadiya, P. Jangir, and A. Kumar, "Moth-flame optimization algorithm for solving real challenging constrained engineering optimization problems," in *Proc. IEEE Students' Conf. Elect., Electron. Comput. Sci. (SCEECS)*, Mar. 2016, pp. 1–5.

[29] Y. Wang, Q. Meng, Q. Qi, J. Yang, and Y. Liu, "Region merging considering within-and between-segment heterogeneity: An improved hybrid remote-sensing image segmentation method," *Remote Sens.*, vol. 10, no. 5, p. 781, 2018.

[30] T. Hershkovitch and T. Riklin-Raviv, "Model-dependent uncertainty estimation of medical image segmentation," in *Proc. IEEE 15th Int. Symp. Biomed. Imag. (ISBI)*, Apr. 2018, pp. 1373–1376.

[31] W. Xiong, J. Xu, Z. Xiong, J. Wang, and M. Liu, "Degraded historical document image binarization using local features and support vector machine (SVM)," *Optik*, vol. 164, pp. 218–223, Jul. 2018.

[32] S. S. Chouhan, A. Kaul, and U. P. Singh, "Soft computing approaches for image segmentation: A survey," *Multimedia Tools Appl.*, vol. 77, no. 21, pp. 28483–28537, 2018.

[33] M. A. El Aziz, A. A. Ewees, and A. E. Hassanien, "Multi-objective whale optimization algorithm for content-based image retrieval," *Multimedia Tools Appl.*, vol. 77, no. 19, pp. 26135–26172, 2018.

[34] M. Mudhsh, S. Xiong, M. A. El Aziz, A. E. Hassanien, and P. Duan, "Hybrid swarm optimization for document image binarization based on OTSU function," in *Proc. CASA*, 2017.

[35] S. Bhattacharyya, P. Dutta, S. De, and G. Klepac, *Hybrid Soft Computing for Image Segmentation*. Cham, Switzerland: Springer, 2016.

[36] S. Eskenazi and P. Gomez-Krämer, and J.-M. Ogier, "A comprehensive survey of mostly textual document segmentation algorithms since 2008," *Pattern Recognit.*, vol. 64, pp. 1–14, Apr. 2017.

[37] K. Tang, X. Yuan, T. Sun, J. Yang, and S. Gao, "An improved scheme for minimum cross entropy threshold selection based on genetic algorithm," *Knowl. Based Syst.*, vol. 24, no. 8, pp. 1131–1138, Dec. 2011.

[38] S. Sarkar, S. Das, and S. S. Chaudhuri, "A multilevel color image thresholding scheme based on minimum cross entropy and differential evolution," *Pattern Recognit. Lett.*, vol. 54, pp. 27–35, Mar. 2015.

[39] H. Gao, Z. Fu, C.-M. Pun, H. Hu, and R. Lan, "A multi-level thresholding image segmentation based on an improved artificial bee colony algorithm," *Comput. Elect. Eng.*, vol. 70, pp. 931–938, Aug. 2018.

[40] D. Oliva, E. Cuevas, G. Pajares, D. Zaldivar, and V. Osuna, "A multilevel thresholding algorithm using electromagnetism optimization," *Neurocomputing*, vol. 139, pp. 357–381, Sep. 2014.

[41] H. Mittal and M. Saraswat, "An optimum multi-level image thresholding segmentation using non-local means 2D histogram and exponential Kbest gravitational search algorithm," *Eng. Appl. Artif. Intell.*, vol. 71, pp. 226–235, May 2018.

[42] W. A. Hussein, S. Sahran, and S. N. H. S. Abdullah, "A new initialization algorithm for bees algorithm," in *Proc. Int. Multi-Conf. Artif. Intell. Technol.* Berlin, Germany: Springer, 2013, pp. 39–52.

[43] A. M. Reynolds, A. D. Smith, D. R. Reynolds, N. L. Carreck, and J. L. Osborne, "Honeybees perform optimal scale-free searching flights when attempting to locate a food source," *J. Experim. Biol.*, vol. 210, no. 21, pp. 3763–3770, 2007.

[44] L. He and S. Huang, "Modified firefly algorithm based multilevel thresholding for color image segmentation," *Neurocomputing*, vol. 240, pp. 152–174, May 2017.

[45] A. K. M. Khairuzzaman and S. Chaudhury, "Multilevel thresholding using grey wolf optimizer for image segmentation," *Expert Syst. Appl.*, vol. 86, pp. 64–76, Nov. 2017.

[46] K. B. Resma and M. S. Nair, "Multilevel thresholding for image segmentation using krill herd optimization algorithm," *J. King Saud Univ.-Comput. Inf. Sci.*, 2018, doi: 10.1016/j.jksuci.2018.04.007.

[47] G. Sun, A. Zhang, Y. Yao, and Z. Wang, "A novel hybrid algorithm of gravitational search algorithm with genetic algorithm for multi-level thresholding," *Appl. Soft Comput.*, vol. 46, pp. 703–730, Sep. 2016.

[48] D. Oliva, S. Hinojosa, E. Cuevas, G. Pajares, O. Avalos, and J. Gálvez, "Cross entropy based thresholding for magnetic resonance brain images using crow search algorithm," *Expert Syst. Appl.*, vol. 79, pp. 164–180, Aug. 2017.

[49] S. C. Satapathy, N. S. M. Raja, V. Rajinikanth, A. S. Ashour, and N. Dey, "Multi-level image thresholding using Otsu and chaotic bat algorithm," *Neural Comput. Appl.*, vol. 29, no. 12, pp. 1285–1307, 2016.

[50] S. Samantaa, N. Dey, P. Das, S. Acharjee, and S. S. Chaudhuri, "Multilevel threshold based gray scale image segmentation using cuckoo search," 2013, *arXiv:1307.0277*. [Online]. Available: https://arxiv.org/abs/1307.0277

[51] V. Rajinikanth, N. S. M. Raja, and S. C. Satapathy, "Robust color image multi-thresholding using between-class variance and cuckoo search algorithm," in *Information Systems Design and Intelligent Applications*. New Delhi, India: Springer, 2016, pp. 379–386.

[52] N. Dey, V. Rajinikanth, A. S. Ashour, and J. M. R. S. Tavares, "Social group optimization supported segmentation and evaluation of skin melanoma images," *Symmetry*, vol. 10, no. 2, p. 51, 2018.

[53] V. Rajinikanth and S. C. Satapathy, "Segmentation of ischemic stroke lesion in brain MRI based on social group optimization and fuzzy-Tsallis entropy," *Arabian J. Sci. Eng.*, vol. 43, no. 8, pp. 4365–4378, 2018.

[54] N. Dey, J. Chaki, L. Moraru, S. Fong, and X.-S. Yang, "Firefly algorithm and its variants in digital image processing: A comprehensive review," in *Applications of Firefly Algorithm and Its Variants*. Singapore: Springer, 2020, pp. 1–28.

[55] V. Rajinikanth and M. S. Couceiro, "RGB histogram based color image segmentation using firefly algorithm," *Procedia Comput. Sci.*, vol. 46, pp. 1449–1457, Jan. 2015.

[56] N. Raja, V. Rajinikanth, and K. Latha, "Otsu based optimal multilevel image thresholding using firefly algorithm," *Model. Simul. Eng.*, vol. 2014, p. 37, Jan. 2014.

[57] V. Rajinikanth, N. S. M. Raja, and K. Latha, "Optimal multilevel image thresholding: An analysis with PSO and BFO algorithms," *Aust. J. Basic Appl. Sci.*, vol. 8, no. 9, pp. 443–454, 2014.

[58] V. Rajinikanth, S. C. Satapathy, S. L. Fernandes, and S. Nachiappan, "Entropy based segmentation of tumor from brain mr images–a study with teaching learning based optimization," *Pattern Recognit. Lett.*, vol. 94, pp. 87–95, Jul. 2017.

[59] N. Otsu, "A threshold selection method from gray-level histograms," *IEEE Trans. Syst., Man, Cybern.*, vol. 9, no. 1, pp. 62–66, Jan. 1979.

[60] L. K. Huang and M. J. J. Wang, "Image thresholding by minimizing the measures of fuzziness," *Pattern Recognit.*, vol. 28, no. 1, pp. 41–51, 1995.
[61] X. Li, Z. Zhao, and H. Cheng, "Fuzzy entropy threshold approach to breast cancer detection," *Inf. Sci.-Appl.*, vol. 4, no. 1, pp. 49–56, 1995.
[62] H. Cheng, Y.-H. Chen, and Y. Sun, "A novel fuzzy entropy approach to image enhancement and thresholding," *Signal Process.*, vol. 75, no. 3, pp. 277–301, 1999.
[63] T. X. Pham, P. Siarry, and H. Oulhadj, "A multi-objective optimization approach for brain mri segmentation using fuzzy entropy clustering and region-based active contour methods," *Magn. Reson. Imag.*, vol. 61, pp. 41–65, Sep. 2019.
[64] E. Sert and D. Avci, "Brain tumor segmentation using neutrosophic expert maximum fuzzy-sure entropy and other approaches," *Biomed. Signal Process. Control*, vol. 47, pp. 276–287, Jan. 2019.
[65] S. Song, H. Jia, and J. Ma, "A chaotic electromagnetic field optimization algorithm based on fuzzy entropy for multilevel thresholding color image segmentation," *Entropy*, vol. 21, no. 4, p. 398, 2019.
[66] D. Oliva, M. A. Elaziz, and S. Hinojosa, "Fuzzy entropy approaches for image segmentation," in *Metaheuristic Algorithms for Image Segmentation: Theory and Applications*. Cham, Switzerland: Springer, 2019, pp. 141–147.
[67] M. A. Elaziz and S. Lu, "Many-objectives multilevel thresholding image segmentation using knee evolutionary algorithm," *Expert Syst. Appl.*, vol. 125, pp. 305–316, Jul. 2019.
[68] S. Mirjalili, "Moth-flame optimization algorithm: A novel nature-inspired heuristic paradigm," *Knowl.-Based Syst.*, vol. 89, pp. 228–249, Nov. 2015.
[69] P. Suganthan, N. Hansen, J. Liang, K. Deb, Y. Chen, A. Auger, and S. Tiwari, "Problem definitions and evaluation criteria for the CEC 2005 special session on real-parameter optimization," Kanpur Genetic Algorithms Lab, IIT, Kanpur, India, Nanyang Technol. Univ., Singapore, Tech. Rep. 2005005, May 2005.
[70] *Berkeley*. Accessed: Nov. 2019. [Online]. Available: https://www2.eecs.berkeley.edu/research/projects/cs/vision/bsds/bsds300/html/dataset/images.html
[71] P.-Y. Yin, "Multilevel minimum cross entropy threshold selection based on particle swarm optimization," *Appl. Math. Comput.*, vol. 184, pp. 503–892, Jan. 2007.
[72] P. Roy, S. Dutta, N. Dey, G. Dey, S. Chakraborty, and R. Ray, "Adaptive thresholding: A comparative study," in *Proc. Int. Conf. Control, Instrum., Commun. Comput. Technol. (ICCICCT)*, Jul. 2014, pp. 1182–1186.
[73] Z. Wang, A. C. Bovik, H. R. Sheikh, and E. P. Simoncelli, "Image quality assessment: From error measurement to structural similarity," *IEEE Trans. Image Process.*, vol. 13, no. 1, pp. 600–613, Jan. 2004.
[74] A. A. Heidari, S. Mirjalili, H. Faris, I. Aljarah, M. Mafarja, and H. Chen, "Harris hawks optimization: Algorithm and applications," *Future Gener. Comput. Syst.*, vol. 97, pp. 849–872, Aug. 2019.
[75] S. Mirjalili and A. Lewis, "The whale optimization algorithm," *Adv. Eng. Softw.*, vol. 95, pp. 51–67, May 2016.
[76] D. Karaboga and C. Ozturk, "A novel clustering approach: Artificial bee colony (ABC) algorithm," *Appl. Soft Comput.*, vol. 11, pp. 652–657, Jan. 2011.
[77] J. Kennedy and R. Eberhart, "Particle swarm optimization (PSO)," in *Proc. IEEE Int. Conf. Neural Netw.*, Perth, WA, Australia, Nov./Dec. 1995, pp. 1942–1948.
[78] M. D. H. F. J. Derrac and S. García, "A practical tutorial on the use of nonparametric statistical tests as a methodology for comparing evolutionary and swarm intelligence algorithms," *Swarm Evol. Comput.*, vol. 1, no. 1, pp. 3–18, 2011.
[79] N. Dey, "Uneven illumination correction of digital images: A survey of the state-of-the-art," *Optik*, vol. 183, pp. 483–495, Apr. 2019.

HUSEIN S. NAJI ALWERFALI received the B.S. degree from Elmergib University, in 2011, the M.S. degrees from the Huazhong University of Science Technology, in 2016, respectively, majored in big data and image analysis, and the Ph.D. degree with the School of Computer Science, Huazhong University of Science and Technology, Wuhan, China. His current research interests include image segmentation and image processing.

MOHAMED ABD ELAZIZ received the B.S. and M.S. degrees in computer science from the Zagazig University, in 2008 and 2011, respectively, and the Ph.D. degree in mathematics and computer science from Zagazig University, Egypt, in 2014. From 2008 to 2011, he was an Assistant Lecturer with the Department of Computer Science. Since 2014, he has been a Lecturer with the Mathematical Department, Zagazig University. He has authored and coauthored more than 70 articles. His research interests include machine learning, signal processing, image processing, and evolutionary algorithms.

MOHAMMED A. A. AL-QANESS received the B.S., M.S., and Ph.D. degrees from the Wuhan University of Technology, in 2010, 2014, and 2017, respectively, all in information and communication engineering. He is currently an Assistant Professor with the School of Computer Science, Wuhan University, Wuhan, China. His current research interests include wireless sensing, mobile computing, machine learning, as well as signal and image processing.

AAQIF AFZAAL ABBASI received the Ph.D. degree in computer engineering from the School of Computer Science and Technology, Huazhong University of Science and Technology, Wuhan, China. He is currently an Assistant Professor with the Department of Software Engineering, Foundation University, Islamabad, Pakistan. His current research interests include parallel and distributed systems, cloud computing, data-intensive computing, and data center performance optimization. He is a member of the ACM.

SONGFENG LU was born in 1968. He received the Ph.D. degree in computer software and theory from the Huazhong University of Science and Technology. He is currently a Professor with the Huazhong University of Science and Technology. His research interests include artificial intelligence, quantum computing, and information security.

FANG LIU received the Ph.D. degree in computer software and theory from the Huazhong University of Science and Technology, in 2002. Her current research interests include AI and machine learning.

LI LI received the Ph.D. degree in mathematics from the Huazhong University of Science and Techbology, in 2007. She is currently an Associate Professor with the Department of Mathematics, Shenzhen University, China. Her current research interests include quantum computing and machine learning.